From the Section of Orthopaedics
Department of Surgical Sciences
Karolinska Institutet, Stockholm, Sweden

DIABETIC OSTEOPATHY

A STUDY IN THE RAT

Tashfeen Ahmad, MD

Stockholm 2003

All previously published papers were reproduced with permission from the publishers.

Paper I was reproduced with permission from Lippincott Williams & Wilkins.
Paper II was reproduced with permission from the Society for Endocrinology.
Figure 1 was reproduced with permission from the Radiological Society of North America

ABSTRACT - DIABETIC OSTEOPATHY. A STUDY IN THE RAT

Tashfeen Ahmad, MD, Dept. of Surgical Sciences, Section of Orthopedics, Karolinska Institutet, Stockholm.

The present study on non-obese Goto-Kakizaki (GK) rats with type-2 diabetes and neuropathy was an attempt to describe and define pertinent features of diabetic osteopathy. Altogether, the study included 33 GK rats aged 12 and 20 months, and 36 age-matched Wistar rats as controls. All underwent test of glucose tolerance and nerve (sciatic) conduction velocity (NCV) showing that the diabetic rats had significantly higher blood glucose levels and lower NCV confirming the presence of diabetes and neuropathy.

Skeletal features Radiologic analysis of bone entailed X-ray, Dual Energy X-ray Absorptiometry (DEXA) and peripheral Quantitative Computed Tomography (pQCT). In diabetic rats, the length of humerus and height of vertebrae was reduced by 8%. The long bones exhibited endosteal erosion of the diaphyses up to 18% and periosteal expansion up to 8%. The vertebrae and metaphyses of long bones showed a decrease up to 24% in areal bone mineral density (BMD), whereas no decrease was seen in the diaphyses. Cross-sectional measurements by pQCT showed a decrease in volumetric BMD ranging from 33 to 62%, which exclusively pertained to trabecular bone (vertebrae, metaphyses), whereas volumetric BMD of the cortical bone of diaphyses was only marginally affected. The results indicate that juxta-articular bone in diabetes is substantially weaker, whereas diaphyseal cortical bone may be even stronger. Over all, the observations suggest that the diabetic skeleton is characterized by regional changes, which cannot be explained by systemic factors like calcium regulating hormones. Local bone turn-over is regulated by complex mechanisms involving cytokines, prostaglandins, growth factors and, also neuropeptides. Further analysis focused on the insulin-like growth factor (IGF) system and neuronal mediators in bone.

IGF system Immunoassays of IGF-I were done on serum, ankle samples and cortical preparations. In addition, the inhibitory IGF-I binding proteins, IGFBP-1 and -4 were analysed in serum. In diabetic rats, serum IGF-I was reduced by 18%, while IGFBP-1 and IGFBP-4 were increased by 89 and 20 %, respectively. This complies with the lower BMD in the diabetic rats. In cortical bone, IGF-I was reduced by 38%, whereas no change was seen in ankles. The loss of IGF-I in cortical bone represents a novel finding. Given the cortical expansion observed in diabetic rats, the opposite was expected. Conceivably, loss of IGF-I results in endosteal erosion, which is compensated by periosteal expansion.

Neuropeptides The analyses focused on two sensory mediators, i.e. substance P (SP) and calcitonin gene-related peptide (CGRP), and one autonomic, i.e. neuropeptide Y (NPY). Immunohistochemistry was applied to ankles and tibial diaphyses, whereas radioimmunoassay (RIA) was used for separate preparations of periosteum, cortex and bone marrow from femur and tibia, whole ankles, dorsal root ganglia (DRG) and lumbar spinal cord. The morphological analysis showed SP, CGRP and NPY positive nerve fibers in bone and joints, which mostly were blood vessel related, although free terminals were also seen. In addition, NPY-positive hematopoietic cells were observed in the bone marrow. RIA revealed a significant decrease of CGRP, albeit not of SP, in DRG (-26%) and spinal cord (-29%) in the diabetic rats. As for bone, only NPY was significantly reduced, most evidently in bone marrow (-66%), but also in cortical bone (-36%) and ankles (-29%). Given the bone anabolic effects of CGRP and NPY, loss of these neuropeptides may prove, at least partly, to underlie the trabecular osteopenia and endocortical erosion observed in diabetic rats.

Conclusion The skeleton of diabetic rats with type-2 diabetes and neuropathy is characterized by regional changes of size, form, mineral content and density and concomitantly with regional abnormalities of the IGF-system and neuropeptides suggesting that also local factors beyond systemic play an important role in the development of diabetic osteopathy.

Key words: Diabetes mellitus type 2, Goto-Kakizaki rat, bone mineral density, insulin-like growth factor-I, insulin-like growth factor binding protein 1, insulin-like growth factor binding protein 4, peripheral neuropathy, substance P, calcitonin gene-related peptide, neuropeptide Y

LIST OF PAPERS

I. Ahmad T, Ohlsson C, Ostenson CG, Kreicbergs A. Peripheral quantitative computed tomography for the detection of diabetic osteopathy. A study in the Goto-Kakizaki rat. Invest Radiol 2003; 38:171-176.

II. Ahmad T, Ohlsson C, Sääf M, Östenson C-G, Kreicbergs A. Skeletal changes in the type-2 diabetic Goto-Kakizaki rat. J Endocrinol 2003; 178:111-116

III. Ahmad T, Ugarph-Morawski A, Lewitt MS, Li J, Sääf M, Brismar K. Diabetic osteopathy and the IGF system in the Goto-Kakizaki rat. Submitted; Aug 2003

IV. Ahmad T, Ugarph-Morawski A, Li J, Indre-Bileviciute-Ljungar, Anja Finn, Östenson C-G, Kreicbergs A. Bone and joint neuropathy in rats with type-2 diabetes. Submitted; Aug 2003

CONTENTS

LIST OF ABBREVIATIONS

|	
DEXA	Dual energy X-ray absorptiometry
PQCT	Peripheral quantitative computed tomography
BMC	Bone mineral content
BMD	Bone mineral density
IGF	Insulin-like growth factor
IGFBP	Insulin-like growth factor binding protein
RIA	Radioimmunoassay
HPLC	High performance liquid chromatography
EDTA	Ethylene diamine tetraacetic acid
IHC	Immunohistochemistry
Cy2	Cyanine-2
SP	Substance P
CGRP	Calcitonin gene-related peptide
NPY	Neuropeptide Y
VIP	Vasoactive intestinal polypeptide

BACKGROUND

The world prevalence of diabetes mellitus is estimated to be around 150 million, out of which 85-95% are being afflicted by the type 2 variant[1]. The prevalence is projected to increase worldwide to 300 million people by 2025[2,3]. Given the high rate of morbidity, the disorder will place a tremendous burden on the health care systems[4]. Among diabetes patients 10-30% have angiopathy, 35-70% retinopathy, 15-40% nephropathy and 60-70% neuropathy[5]. In addition to these classical complications, accumulating data suggests that diabetic patients are at increased risk of developing osteopathic changes, although the nature and prevalence of this complication are still a matter of dispute.

DIABETIC OSTEOPATHY

Today it is widely recognized that patients with diabetes have an increased risk of sustaining fractures[6,7]. Diabetes is also associated with impaired fracture healing; the fracture callus in diabetes is slow to appear and mature, and there is a high rate of non-unions[8]. In diabetic animals, the fracture callus is weaker than normal[9]. The decreased mechanical strength has been attributed to decreased collagen synthesis[9]. Clinically, it is also well known that the complication rate of fracture treatment in diabetes is elevated because of increased susceptibility to infections, non-union, implant failure and re-dislocation, sometimes even prompting amputation. Altogether, it now seems well established that patients with diabetes have a higher incidence and morbidity from fracture as compared to non-diabetic subjects. In addition, clinical diabetes is associated with an increased incidence of spontaneous collapse of subchondral bone in load-bearing joints and development of Charcot arthropathy[10] (Fig.1).

In diabetes, abnormalities of the endocrine organs such as the hypothalamus, pituitary, adrenal, thyroid, parathyroid and the gonads as well as the endocrine function of the adipose tissue and the vitamin D system have been reported[11]. However, it is unknown to what extent each of these disorders affects bone turn-over in diabetes. Most studies on diabetic osteopathy suggest that it is a form of low turn-over osteoporosis without hyperparathyroidism or osteomalacia[12-16], though increased bone resorption has also been reported[17].

Figure 1 (A-C). Diabetic osteopathy
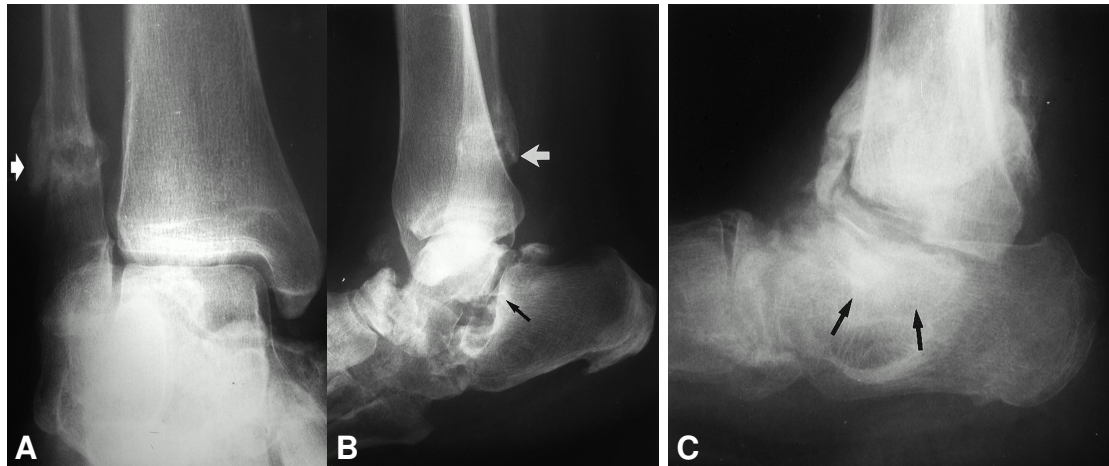
Spontaneous fracture of the fibula and neuropathic osteoarthropathy of the foot in a 63-year-old diabetic woman. Anteroposterior (A) and lateral (B) radiographs of the ankle show disruption of the subtalar joint (black arrow in B), talonavicular subluxation, and fracture of the distal fibula (white arrow in A and B). The lateral radiograph (C) depicts neuropathic osteoarthropathy of the ankle and hindfoot in a 42-year-old diabetic man. The distal tibia is resorbed and has sharp margins resembling surgical amputation. The talar dome is resorbed. Sclerosis is present, and subtalar joints (arrows) can no longer be identified.Pictures are copyright of RadioGraphics Online (http://radiographics.rsnajnls.org/) and are reproduced with permission from the Radiological Society of North America.

Taken together it appears that bone in diabetes is different from normal. The above features are often referred to as "diabetic osteopathy". However, the exact nature of this disorder has so far not been well defined, nor have the underlying mechanisms been clarified. This may explain why there is still a lack of consensus about diabetic osteopathy, despite substantial evidence pointing to its existence. To some extent, this can be explained by lack of appropriate definitions of the pertinent features of the disorder. This in turn can be ascribed to differences in the variables considered and methodologies employed.

ANALYTIC APPROACH

By far the commonest non-invasive method for assessment of bone structure is dual energy X-ray absorptiometry (DEXA), which is routinely used to evaluate osteoporosis[18]. In the diabetic population, bone densitometric studies have revealed a lower than normal bone mineral density. However, findings on BMD vary between type-1 and type-2 diabetes. In type-1 diabetes, most studies show a lower bone mineral density (BMD), but in type-2 diabetes lower, normal and even higher BMD has been reported[19-21]. The increased BMD in type-2 diabetes primarily

pertains to the lumbar vertebrae, while peripheral sites such as femoral neck and distal radius frequently exhibit a lower BMD. Thus, type of diabetes seems to be one determinant of the bone changes, but the difficulties in obtaining conclusive data on diabetic bone are also due to confounding factors such as treatment and obesity.

Insulin therapy is likely to increase BMD because of its effect on bone[22]. Indeed, patients treated with insulin have been shown to exhibit higher BMD than those with oral hypoglycemic agents[23]. Obesity, more common in type-2 diabetes, is likely to protect against osteopenia since body mass index correlates with BMD and bone size. Thus, osteopenia due to the diabetes may be offset by the gain of BMD due to obesity, thereby resulting in a normalized BMD.

The lack of coherent data on bone in diabetes may also be attributed to the shortcomings of the methodology commonly employed, i.e. DEXA. Thus, the method merely provides areal bone mineral density (a-BMD) from projected X-ray images. A large amount of age, gender and race-specific data on a-BMD in healthy population is available, mainly for the lumbar spine, proximal femur and distal radius. Significant deviations from these findings are considered to reflect osteoporosis[18]. However, the conventionally used protocols and reference data may not be appropriate for osteopathic conditions other than osteoporosis. A-BMD measurements are highly dependent on bone size[24]. Thus, growing children exhibit a progressive increase in a-BMD just because the bones get longer and wider. As DEXA is based on projected radiographic images, it is not well suited for separate analysis of cortical and trabecular components of bone. In these respects, the more recently introduced quantitative computed tomography (QCT) technique is superior. It provides "true" volumetric BMD (v-BMD) independently of bone size. Notably, the v-BMD of cortical bone has been found to be essentially constant from childhood until middle age, but decreased in old age[25,26]. pQCT also permits separate determination of BMD of cortical and trabecular compartments in defined regions of a given bone[27]. Thus, for bone assessment in diseases affecting specific bone sub-regions, pQCT is likely to be superior to DEXA, and this may be true for diabetic osteopathy as well. So far, however, this has not been explored.

MECHANISMS

The pathomechanisms behind the skeletal changes observed in diabetes essentially remain unknown. It is reasonable to assume that they somehow are related to insulin deficiency. Insulin is a growth factor for cartilage and bone[28,29], acting through a variety of mechanisms. In type-1 diabetes an absolute deficiency of insulin exists. In patients with type-2 diabetes, a relative deficiency exists due to peripheral insulin resistance and an impaired insulin release in response to glucose load, while absolute levels are normal or elevated. Notably, hyperglycemia has been shown to impair osteoblast proliferation both directly and indirectly[17,30]. Evidence for the indirect effect comes from observations of decreased sensitivity of osteoblasts to the effect of growth factors in the presence of hyperglycemia[31,32].

IGF Insulin-like growth factors (IGF) have been shown to have important effects on bone[33-37]. The first IGF to be characterized, i.e. IGF-I, is a single-chain polypeptide of 70 amino acids produced by liver cells, but also by several other cell-types including osteoblasts[38,39]. It is called "insulin-like" because it bears structural homology to proinsulin, and has affinity for the insulin receptor. IGF-I also has a specific receptor of its own (IGF-I receptor). IGF-I under normal conditions is anabolic for bone[33-37]. IGF-I gene deletion leads to severe osteopenia and growth retardation[40]. In IGF-I receptor knockout mice, significant reduction in trabecular bone mass and deficient mineralization is seen, though growth of the bone is normal[41]. The effect of IGFs is modulated by certain proteins, known as IGF binding proteins (IGFBPs). To date, six different IGFBPs have been characterized. Apart from modulating IGF-I action[42], IGFBPs also have direct effects on osteoblasts[43,44] and osteoclasts[45]. In general, IGFBPs bind to IGF-I and reduce its bioavailability and thereby its action. In diabetes mellitus, low serum and tissue levels of IGF-I have been demonstrated[46,47], but data on bone is sparse. It is quite conceivable that an abnormality of the IGF system underlies diabetic osteopathy. Whether the IGF-system also indirectly causes osteopathy through other pathways is unknown.

Angiopathy In the feet of diabetic patients, increased blood flow associated with arterio-venous shunting[48], and increased bone blood flow[49] have been demonstrated, most likely due to autonomic neuropathy causing

disturbed vasoregulation. Notably, increased bone resorption has been observed in the presence of increased blood flow[50,51]. Arterio-venous shunting deprives the tissues of oxygen and nutrients even though blood flow may appear to be increased. One of the main theories on the mechanism underlying Charcot joint formation, the neuro-vascular theory, considers osteopenia to be a result of disturbed vasoregulation caused by neuropathy[52].

Bone neuropathy In disorders of both the central nervous system such as paraplegia[53] and head injury[54,55] as well as those of the peripheral nervous system such as diabetic neuropathy[56] and leprosy[57] abnormal fracture healing and focal abnormalities of bone are observed. Peripheral neuropathy in diabetes is a common observation. Notably, it is a consistent feature of diabetic patients developing osteopathy. Neuropathy may affect bone through abnormal vasoregulation, but probably also has direct effects on bone.

Bone innervation The first reports on bone innervation according to specific transmitters, i.e. neuropeptides, were published in the late 80's by Bjurholm et. al[58,59]. Using immunohistochemistry, both sensory and autonomic nerve fibers in bone were identified. Most of the nerve fibers were found in areas of high osteogenic activity, i.e. along the osteochondral junction of the epiphyseal plate and the periosteum[60]. The nerves have been shown to contain a variety of neuronal mediators, including sensory, autonomic, opioid and immune-related peptides[61]. Originally, nerves in bone were considered mainly to have a sensory and vasoregulatory role. However, over the last couple of decades direct effects on bone tissue have been observed for several neuronal mediators, notably, so-called neuropeptides. Among sensory neuropeptides, substance P (SP) has a bone resorptive action[62,63] while calcitonin gene-related peptide (CGRP) inhibits resorption[64] and suppresses osteoclast formation and proliferation[65,66]. The SP receptor, i.e. neurokinin-1 (NK-1), has been demonstrated in osteoblasts, osteocytes and osteoclasts[67], and evidence of their function has also been reported[68-70]. The autonomic neuropeptide vasoactive intestinal polypeptide (VIP) acts on both osteoclasts and osteoblasts and has a bone-resorptive effect[71]. Via the central nervous system, another autonomic neuropeptide, i.e. neuropeptide Y (NPY), exerts an anti-osteogenic effect[72]. In the peripheral nervous system, NPY appears to have a pro-osteogenic

effect. It is co-released with noradrenaline from sympathetic nerves, and sympathectomy by surgical[73] or chemical[74] methods increases osteoclast number and surface. Moreover, NPY modulates osteoblastic response to noradrenaline as well as parathyroid hormone through a receptor-receptor interaction[68,69] *in vitro*. Thus, it is reasonable to assume that altered expression of neuropeptides in disorders of the peripheral nervous system adversely affects bone. As for indirect effects, interactions between neurotransmitters on one hand and growth factors and cytokines on the other are well known[75,76].

Neuropathy and osteopathy Presumably, neuropathy can cause osteopenia through dysregulation of the direct neuropeptidergic effects on bone and/or disturbance of their indirect effects via growth factors and cytokines. Altogether, it is quite conceivable that diabetic neuropathy underlies diabetic osteopathy. Diabetic neuropathy is a broadly used term which is defined differently by people from different fields. Thus, the clinician defines it according to the signs and symptoms of the patient, and a variety of elaborate definitions and clinical tests have been advocated in the literature[77,78]. The electrophysiologist defines it e.g. by nerve conduction velocity, action potential amplitudes and latencies. The pathologist defines it according to nerve morphology. Classical findings include axonal degeneration (nerve cells) and demyelination (Schwann cells)[79]. However, for bone an important aspect may be the peripheral occurrence of neuronal mediators. Notably, in clinical and experimental studies on diabetes a decrease of neuropeptides has been demonstrated in tissues such as dorsal root ganglia[80], sciatic nerve[80,81], skin[82] and plasma[83]. However, to our knowledge no study has been conducted to analyze the occurrence of neuropeptides in bone and joints in diabetes. Thus, "bone and joint neuropathy" from this perspective has so far not been defined. Although, this approach cannot provide a clinical definition, it may contribute to a better understanding of the pathomechanisms of neuropathy and hopefully, also, to the development of new therapy.

HYPOTHESES AND AIMS

Based on the hypothesis that osteopathy in diabetes exhibits typical skeletal features, which may be caused by abnormalities of the IGF-system and the nervous system in bone and joints, the present study included the following aims:

1. Identify the most appropriate radiological method for assessment of diabetic osteopathy

2. Describe radiologically the typical skeletal features of diabetic osteopathy

3. Assess the systemic as well as the local bone and joint status of the IGF system in diabetic osteopathy

4. Explore and define abnormalities of the peripheral nervous system in diabetic osteopathy according to neuropeptide occurrence in bone and joints

STUDY DESIGN

Total number of rats = 33 diabetic Goto-Kakizaki + 36 control Wistar

20 month

12 month

Paper I

10 GK + 10 W

Diabetes
Glucose tolerance

Bone mineral and Dimensions
   DEXA
   pQCT
   Ash weight
     Tibia
     Metatarsal

Paper II

5 GK + 5 W

Diabetes
Glucose tolerance

Bone mineral and Dimensions
   pQCT
     Humerus
     Vertebrae
     Tibia
     Metatarsal

Paper III+IV

18 GK + 21 W

Diabetes
Glucose tolerance

Neuropathy
Nerve conduction

Bone mineral
   DEXA
     Humerus
     Vertebrae
     Tibia

Immunoassays
   Insulin
   IGF system
     Serum
   IGF-I
     Cortical bone
     Joint
   Neuropeptides
     Cortical bone
     Ankle
     Neural tissue

Immunohisto-chemistry
   Neuropeptides
     Cortical bone
     Ankle
     Spinal cord
     Dorsal root
       ganglia

MATERIAL

ANIMALS

The study included 33 Goto-Kakizaki (GK) rats[84] with spontaneous type-2 diabetes mellitus aged 12 months (Paper II-IV) and 20 months (Paper I), respectively. The GK rats were taken from our colony bred under supervision of the Department of Endocrinology and Diabetology at the Karolinska Hospital. The control group comprised of age-matched female Wistar rats (B&K Universal, Stockholm, Sweden) with normal glucose tolerance. The 12-month old rats were female while the 20-month old rats were male. The GK rat[85] was originally developed from the Wistar strain by selective inbreeding on the basis of impaired glucose tolerance. Thus, Wistar rats are the only relevant controls.

Comments An animal model was chosen because of the intention to analyze neuronal mediators and IGF in bone and joint tissue. A human study, which would entail biopsy specimens from bone and joints, was not considered ethically justifiable because of the inconvenience and risk of infection and other complications. *In-vitro* experiments were not an option since the study required an intact nervous system and a functional IGF axis.

The rationale of choosing a model of type-2 diabetes instead of type-1 pertained to insulin deficiency as a confounding factor. Most models of type-1 diabetes as opposed to type-2 require insulin treatment for survival over a long period. Since insulin is a strong trophic factor for bone[22], both it's deficiency as well as treatment would have been a major confounding factor for this study in which osteopenia was an outcome parameter. Moreover, the prevalence of type-2 diabetes is greater than that of type-1[1].

The GK rats exhibit mild to moderate hyperglycemia with onset early after birth[86]. They have normal or slightly elevated plasma insulin levels in the fed state, mild hypoinsulinemia in the fasting state and impaired insulin response to glucose. The animals develop the chronic complications of diabetes including angiopathy and nephropathy even though the metabolic abnormality is not severe. Also, the conduction velocity of peripheral nerves progressively declines with age, and the morphological changes in the nerves are very similar to those seen in human diabetic neuropathy[87].

The GK-rat is not obese, unlike other rat models of type-2 diabetes. Thus, it may reveal effects of diabetes on bone that could be masked otherwise by obesity seen in other rat models e.g. Zucker diabetic fatty rat[88], and in humans with type-2 diabetes. The appropriateness of this animal model for the study of osteopathy and neuropathy has been reported previously[89]. In human type-2 diabetes obesity is common. However, in the experimental setup it is an advantage to have a lean model, since obesity can increase bone mass, and thereby mask the effect of diabetes.

Housing and care The animals were housed in cages with up to four rats in each cage, and cared for according to the animal department's protocol. The same diet, standard rat-chow, was provided *ad-lib* to both diabetic and control rats. No treatment was given to the diabetic rats to correct the diabetes, since such treatment would affect bone turn-over. Notably, insulin is a growth factor for bone. Since GK rats are not obese, dietary restriction would lead to under-nutrition, and thereby impair bone formation.

Anesthesia and euthanasia Anesthesia for *in-vivo* investigations was performed with intraperitoneal injection of Hypnorm®. For immunohistochemistry, animals underwent *in-vivo* perfusion fixation through the left heart, under sodium-pentobarbitone anesthesia, then killed for sample collection. For all other methods, they were killed by decapitation under pentobarbitone overdose.

Ethics All animal experiments were performed with approval from the Ethics Committee for Animal Research (North Stockholm, Sweden). Animals were euthanized in accordance with the guidelines of the Central Animal Research Committee[90].

Body Weight This variable was considered to permit valid conclusions of bone data. As can be seen from Table 1 the diabetic rats exhibited a lower body weight compared to controls. This difference between diabetic and Wistar rats was more pronounced in the older group of male rats than the younger group of female rats. These data were taken into account in the analysis of different bone features.

**Table 1. Body weight expressed as mean (g) ± SD.**

	Control	Diabetes	Difference (p-value)
12 month (n=26+23)	294 ± 32	268 ± 23	-9% (*0.002*)
20 month (n=10+10)	645 ± 103	454 ± 31	-30% (*<0.001*)

Diabetes To assess the diabetic status of the GK-rats, an intraperitoneal (i.p.) glucose tolerance test was done[85]. The animals were fasted overnight and fasting glucose was measured in tail blood. An i.p. injection of glucose solution (2g/kg body weight) was given, then blood glucose was measured after 30 and 120 min of glucose injection. Glucose levels were determined using a portable blood glucose analyzer (Accutrend®, Boehringer Mannheim, Mannheim, Germany). Both 12 and 20 months diabetic rats as well as Wistar rats were included in the test. As can be seen from Fig 2, the diabetic rats had significantly higher blood glucose levels confirming the presence of diabetes.

Figure 2. Glucose tolerance test
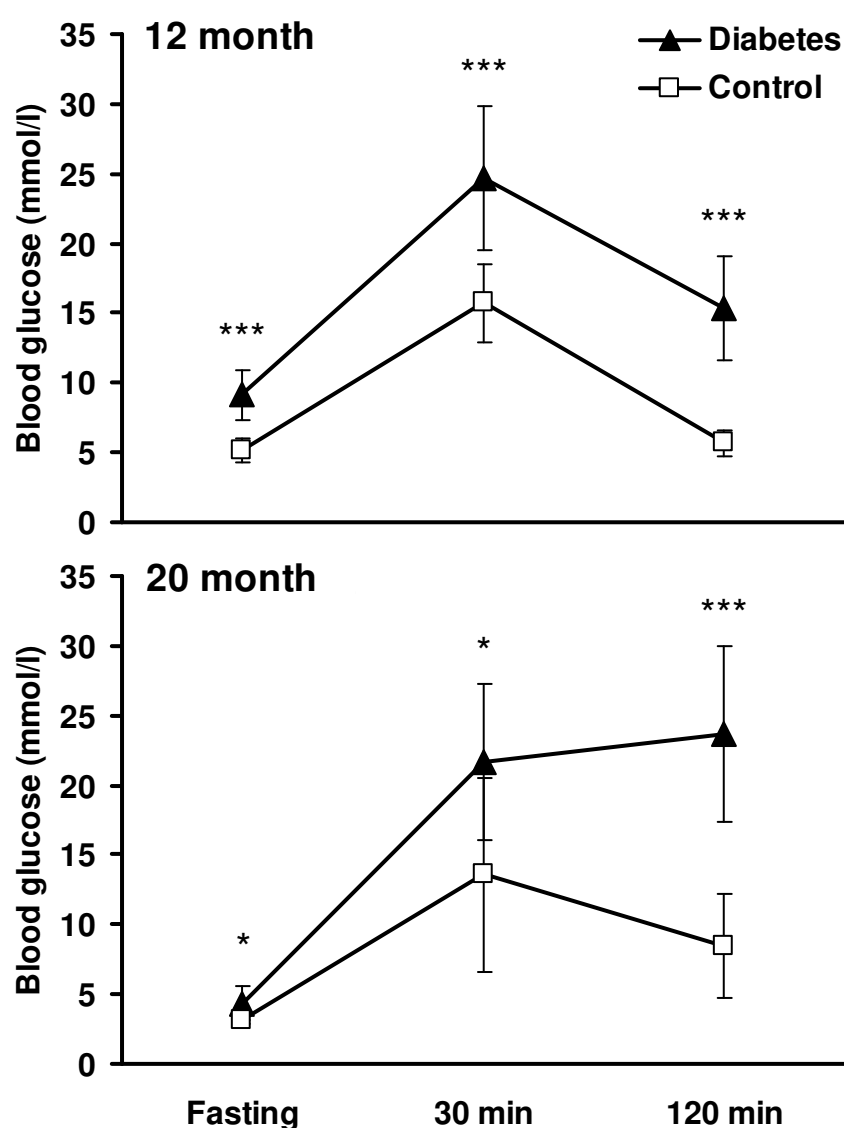
Neuropathy In both 12 and 20 months old diabetic rats as well as Wistar rats nerve conduction velocity (NCV) was determined The rats were anesthetised with an intraperitoneal Hypnorm® (Janssen, Beerse, Belgium) injection (0.5 ml/kg bw). Sciatic NCV was measured using Neuropack 2 Evoked Potential Measuring System (Nihon Kohden Corporation, Tokyo, Japan), employing needle electrodes. The nerve was stimulated at the sciatic notch, while recording was made from the hind-paw. The distance between the stimulating and recording electrode, and the latency between the electrical stimulation and the first observed action potential were used to determine nerve conduction velocity. Table 2 shows that the mean NCV was reduced in the diabetic rats.

Table 2. Nerve conduction velocity results from 12- and 20-month old rats expressed as mean ± standard deviation.

	Control n=36	Diabetes n=33	Difference (p-value)	
12 month	70.9 ± 4.3	59.1 ± 2.9	-16.7%	(<0.001)
20 month	61.8 ± 4.9	49.8 ± 5.1	-24.1%	(<0.001)

TISSUES

The study focused on bone and joints using a variety of different *in-vivo* and *ex-vivo* methods. The radiologic investigations were applied to the whole skeleton, but also to individual bones, i.e. humerus, tibia, 3rd metatarsal and the lumbar vertebrae (L4-5). The same individual bones were also subjected to ash weight determinations. Immunohistochemistry for neuropeptides was applied to tibia, ankle, spinal cord and dorsal root ganglia. Immunoassays for tissue concentrations of neuropeptides were applied to separate samples of periosteum, bone marrow and cortical bone from femur and tibia, and also to whole ankle joints, dorsal root ganglia and spinal cord (L2-5). Preparations of cortical bone from femur were also made for immunoassay of IGF-I. Finally, blood samples were taken for determining the concentration of glucose, insulin, IGF-I and IGFBP-1 and IGFBP-4.

METHODS

RADIOGRAPHY

X-rays of the tibia and humerus were taken under Hypnorm® anaesthesia. A Siemens dental X-ray machine (Heliodent DS, Siemens AG, Bensheim, Germany) was used. It has a 70 micron focal spot, and fixed power and voltage at 7mA and 60 kV, respectively. Dental radiographic films of size 8.5 x 5.4 cm from Kodak (Ektaspeed Plus, Eastman Kodak, Rochester, NY, USA) were used. After a series of trials, it was possible to achieve an optimum X-ray image with a 33% magnification by keeping the film 25 cm away from the rat and the rat 75 cm away from the X-ray source with the use of a specially designed platform. With this configuration, an exposure time of 1.25 sec proved adequate. Lateral X-rays of the limbs were taken, X-rays were developed and then digitized using a HP Scanjet II scanner (Hewlett-Packard, Singapore). Scanned images were printed at a magnification of 20X and the outer (periosteal) diameter and the inner (endosteal) diameter of the bone were measured in the distal third of the diaphysis with a precision caliper. Cortical thickness and cortical thickness index were calculated as follows:

$$\text{Cortical thickness: } \frac{Outer - Inner}{2} \qquad \text{Cortical thickness index: } \frac{Outer}{Inner}$$

Two observers independently made the measurements, from which the mean was calculated. The correlation between two observers was R=0.65 and inter-observer variation was 9%.

DEXA

Analysis of bone mineral content and density was done using dual energy X-ray absorptiometry (DEXA). This method has previously been validated for assessment of bone mineral content in rats[91,92]. DEXA was done *in-vivo* on rats from which bone samples were to be processed for neuropeptide and IGF-I assays, while in the remaining it was done *ex-vivo*. The *in-vivo* analysis was done under Hypnorm® anaesthesia in a fan beam X-ray bone densitometer (QDR 4500A, Hologic, Bedford, MA, USA) at the Department of Radiology, Karolinska Hospital, Stockholm. The machine was calibrated daily with a phantom provided by the manufacturer. Whole body scans and regional high-resolution scans of the humerus, lumbar vertebrae L4 and L5 and the tibia were performed.

The software permits analysis of defined regions within the bones. Hence, for humerus and tibia, the metaphysis and diaphysis were analysed

separately. For tibia, the sub-regions included the metaphysis in the proximal 15% of the bone length and the diaphysis in the distal 15%. For humerus, the corresponding sub-regions were proximal 20% and middle 15%. The vertebrae L4 and L5 were analysed together as a whole. Analysis provided projected bone area in cm^2, bone mineral content (BMC) in grams and areal bone mineral density (a-BMD) in grams per cm^2.

For *ex-vivo* analysis, the rats were killed by decapitation under anaesthesia with Hypnorm®. The lumbar vertebrae including part of the pelvis, whole humerus, tibia and 3rd metatarsal bones were dissected, cleared of soft tissue and stored in 70% ethanol. A high-resolution peripheral DEXA (pDEXA) machine was used (pDEXA Sabre, Norland, Fort Atkinson, WI, USA)[93]. This machine, as well as the pQCT machine (see below), are located in the animal laboratory of the Department of Endocrinology, Sahlgrenska University Hospital, Gothenburg, Sweden. It is calibrated daily with a phantom provided by the manufacturer. Bones were placed in a petri-dish containing a 15 mm layer of 70% ethanol. Medium-resolution scans were taken with the settings at line spacing 0.5 mm, speed 15 mm/sec and histogram averaging width 0.2 g/cm^2. The length of the bones was measured using the software's ruler tool, which has a precision of 0.1 mm. Sub-region selections were done in the same way as for *ex-vivo* DEXA. Bone area, BMC and BMD were obtained for whole bones and the sub-regions described.

The inter-scan coefficient of variation (CV) for the DEXA measurements was 3-5%, as assessed by scanning bones five times after repositioning.

PQCT

Tomographic measurements of the same post-mortem specimens were made using the Stratec XCT Research M (Norland, Fort Atkinson, WI, USA), which has a voxel resolution of 70 microns, and software specifically modified for use on small bone specimens (version 5.40B, Stratec)[94].

The bones were placed in plastic tubes filled with 70% ethanol. For trabecular bone analysis of the long bones, they were scanned at the proximal metaphysis. To determine the most suitable level a series of scans was performed at different distances from the proximal growth plate line. A distance equal to 4% of the whole bone length for tibia and 15% for humerus was chosen, considering the amount of trabecular bone. These sites, well within the metaphysis, were chosen for trabecular BMD analysis. In the metatarsal, no metaphyseal scan was taken for technical reasons because of the small size of the bone and very short metaphysis. In the spine, a series of scans was done on the L4 and L5 vertebral bodies, and two levels were chosen; the mid-portion (50% of vertebral body height) and near the distal end-plate (85% of height) (Fig.3).

Figure 3 A-D. pQCT
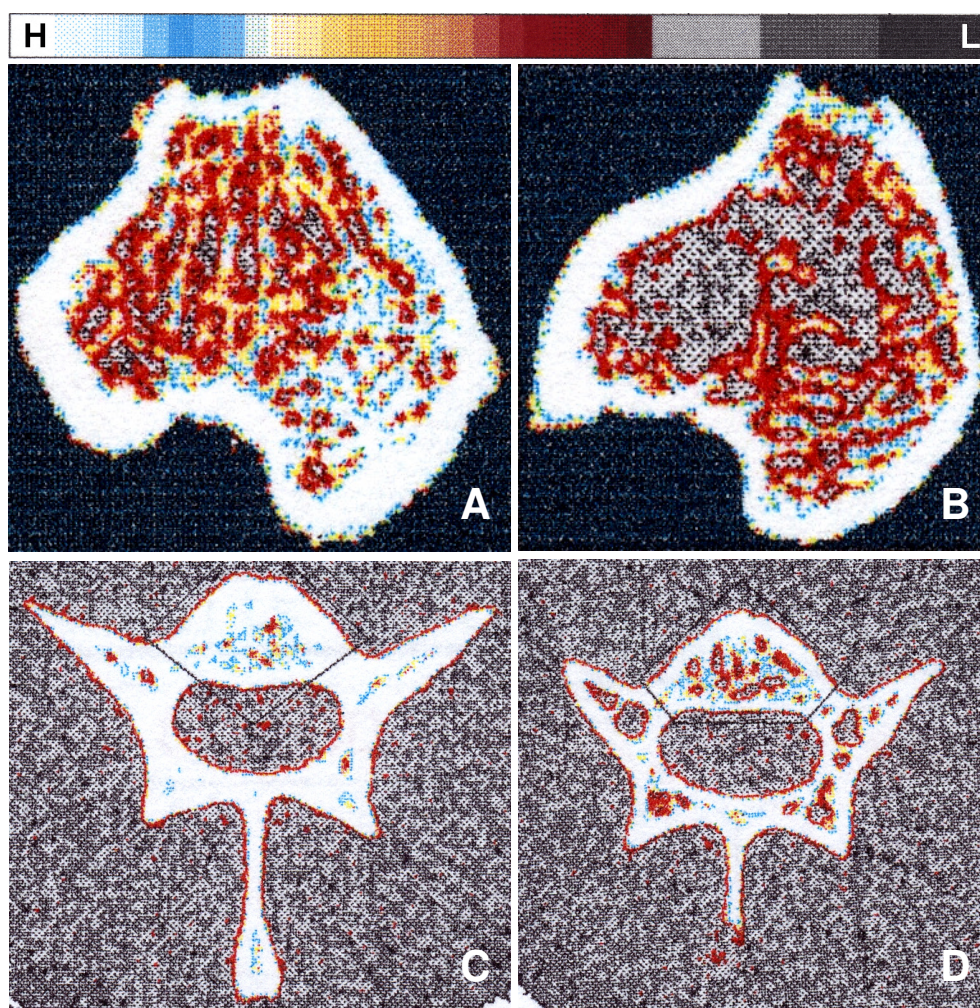
PQCT pictures from proximal tibia (A,B) and vertebral bodies (C,D) from control (A,C) and diabetic (B,D) rats. Lower BMD in the trabecular regions can be observed in diabetic rats. H=high BMD, L=low BMD

For identifying trabecular bone the area protocol was selected, which defines trabecular bone as that lying within the inner 45% of the cross sectional area. This protocol is a standard in the CT software and a convention applied by others[95,96]. Analysis gave the cross-sectional area in mm^2 and volumetric BMD (v-BMD) in g/cm^3 for the whole cross-section as well as separately for the trabecular bone. For cortical bone analysis of diaphyseal bone, the humerus was scanned at 70% of its length from the proximal end, the tibia at 75% from the proximal end, and the metatarsal in its middle. These positions were chosen because they lie within the cylindrical portions of the bones, where variations in bone dimension due to positioning are minimal.

For identifying cortical bone, the software uses density thresholding and calculates periosteal and endosteal diameters based on the "circular ring

model"[97]. Analysis provides volumetric cortical BMD in g/cm^3, cortical thickness in mm, periosteal and endosteal circumferences in mm, and cross-sectional moment of inertia in mm^4, the latter an estimate of bending strength. The bending strength and/or stiffness of long bones is related to both cross-sectional moment of inertia and Young's elastic modulus[98]. The former indicates the architectural fitness and depends on the external diameters of bone cross section, while the latter represents bone material stiffness and is related to tissue ash weight content per dry weight, i.e. BMD.

The inter-assay coefficients of variation (CV) for the pQCT measurements, assessed previously in our laboratory by scanning bones five times after repositioning, was less than 2%.

Comments When analyzing bone size and form, DEXA and pQCT analyses offer different information. DEXA software provides 2-dimensional data from X-ray images, based on the X-ray absorption characteristics of mineralized tissues. It is able to assess the size of the whole skeleton and of individual bones in terms of projected area. Also, within individual bones analysis of sub-regions is possible by defining of regions of interest from the software[99]. The main use of DEXA is in the assessment of areal BMD. The software calculates a-BMD by dividing the BMC with the bone area. Many studies have shown good correlation between a-BMD measurements from DEXA and bone strength as well as fracture risk[100]. It has now become a fairly routine procedure in the clinical setting for evaluation of osteoporosis and response to therapy[18].

In contrast to DEXA, pQCT offers 3-dimensional information. It is based on cross-sectional slices with a pre-determined volume. It determines BMC from tomographic data, and calculates BMD by dividing the content with the volume of bone. The BMD thus obtained is mineral per unit volume of bone, representing volumetric "true" BMD. pQCT permits the assessment of circumferential morphology and is able to distinguish between cortical and trabecular bone[93]. It has been validated against histomorphometrical analysis of trabecular and cortical bone[101-103].

ASH WEIGHT

Ash weight analysis is used as a gold standard to validate BMC measurements by DEXA[104]. After the DEXA and pQCT analyses, the post-mortem specimens were defatted in acetone for 48 hours and desiccated at 60ºC for 72 hours. Defatted dry weight of the bones was measured. The long

bones were divided into metaphyseal and diaphyseal portions, corresponding roughly to the sub-regions selected in DEXA software. The vertebrae L4 and L5 were disarticulated from the rest of the spine. Each bone and segment of bone was weighed, incinerated at 700°C in a muffle furnace (MR 170, Axel Kistner, Stockholm, Sweden), and then ash weight (mg) was determined reflecting mineral content. The sum of ash weights of the segments of each bone gives the total mineral content of that bone. When ash weight is divided by the dry defatted weight, it indicates the proportion of the dry weight of the bone that is mineral as opposed to matrix. This percent ash is another estimate of mineral density.

IMMUNOHISTOCHEMISTRY

Immunohistochemistry (IHC) was done for morphological analysis of nerve fiber occurrence and distribution according to specific neuropeptides in bone and joint tissue.

The rats were anesthetized with Hypnorm® and perfused through the left heart with phosphate-buffered saline (PBS) while being exsanguinated through the right atrium, until the effluent from the atrium was nearly clear of blood (approx 300 ml PBS). Perfusion fixation was then done with Zamboni's fixative (4% paraformaldehyde with picric acid)[105] until the extremities became yellow and stiff (approx 300 ml).

The tibial diaphysis, ankles, the L2-L5 segment of the spinal cord and the corresponding dorsal root ganglia were dissected. Samples were stored in Zamboni's fixative for post-perfusion fixation for 6-8 hours, then the soft tissue samples were placed in buffered 20% sucrose while the skeletal samples were demineralized in 4% buffered EDTA solution[106]. Twice weekly exchanges of the solution were done for a period of approx. 4-6 weeks, until adequate demineralization was confirmed by passing a needle through different parts of the bones, then the samples were placed in 20% sucrose. After having been at least 48 hours in sucrose, the samples were embedded in Tissue-Tek® O.C.T. compound (Sakura Finetek, the Netherlands). Frozen sections were made on a Leitz® 1720 cryostat (Ernst Leitz, Wetzlar, Germany) at 15 µm thickness and transferred onto SuperFrost® Plus glass slides (Menzel-Glaser, Freiberg, Germany).

The slides were stained according to the avidin/biotin system of immunostaining. Commercially available polyclonal antibodies against two sensory neuropeptides i.e. substance P (SP) and calcitonin gene-related peptide (CGRP), and one autonomic i.e. neuropeptide Y (NPY) (Peninsula

Labs., St. Helens, UK) were applied to the sections and incubated overnight. The SP antibodies cross-react with neurokinin A (40%), but not with endothelin 1. The CGRP antibodies cross-react with rat CGRP II (79%) but not with amylin, calcitonin or somatostatin. The NPY antibody does not cross react with PYY, pancreatic polypeptide, VIP, amylin, insulin or somatostatin. The dilutions were 1:10000 for SP and CGRP, and 1:5000 for NPY antiserum. Incubation was then done with biotinylated secondary antibodies for 40 minutes. Finally, the bound secondary antibodies were labeled with the fluorochrome Cyanine-2 (Cy-2) -conjugated avidin (Amersham Biosciences, Uppsala, Sweden) diluted 1:2000, during 40 minute incubation. Control staining was performed by omitting the primary antibody.

The slides were mounted with cover slips using glycerol gelatin and visualized under an epifluorescence microscope (Eclipse E800, Nikon, Tokyo, Japan) connected to a computer via a Nikon DXM1200 digital video camera.

RIA - NEUROPEPTIDES

Quantitation of neuropeptides in tissue extracts was done by RIA. Under Hypnorm® anesthesia, the animals were decapitated and blood was collected, centrifuged and serum was frozen. Both ankles were dissected and crushed. From the diaphyses of both femora and tibiae, the periosteum, bone marrow and cortical bone were collected. The periosteum was scraped off from the bone, the marrow was pushed out from the medullary canal and the remaining cortical bone was crushed. The lumbar spinal cord and dorsal root ganglia were also collected, as mentioned for immunohistochemistry. Wet weight of the samples was measured using a precision balance. Samples were frozen in a box of dry ice and subsequently stored in a –70ºC freezer. Throughout dissection samples were kept on petri-dishes containing ice.

Extraction from the frozen samples was done by boiling the soft tissues in 1M acetic acid and skeletal tissues in 2M acetic acid in 4%EDTA for 10 minutes[107,108]. Samples were homogenized with Polytron® and sonicated, then centrifuged at 3,000 RPM for 15 min at 4ºC. The supernatant was frozen at –70ºC and subsequently lyophilized.

Samples for neuropeptide analysis were reconstituted in phosphate buffer and assayed by competitive radioimmunoassay. The samples and standard peptides were incubated with rabbit antibodies directed against SP and

CGRP (courtesy Prof. E. Theodorson, Linköping University, Sweden)[109] and NPY (Phoenix, CA, USA) for 48 hours at 4ºC. The SP antibodies cross-react with SP sulfoxide, but not with other tachykinins. The CGRP antibodies cross-react with CGRP α (93%) and β (24%), but negligibly (<0.01%) with SP, NPY and other peptides. The NPY antibodies cross-react with PYY (100%) but not with VIP, amylin, insulin or somatostatin. Radioiodine (^{131}I)-labeled peptide was added and incubation done for 20-24 hrs.

To separate the bound and unbound radioligand, Sac-Cel® (Wellcome Diagnostics/IDS, Boldon, England) for SP and CGRP and decanting Suspension-3 (Pharmacia and Upjohn Diagnostics, Uppsala, Sweden) for NPY were added. The reaction was stopped after 30 minutes by adding distilled water, tubes were centrifuged at 6-8ºC at 3500 RPM for 15 min, and the supernatant containing the unbound radioligand was decanted.

The radioactivity in the residual pellets was measured using a gamma counter (Wallac Inc., Turku, Finland). The concentrations of neuropeptides in pmol/L of the sample preparation were calculated by the Gamma counter's computer software. The detection limit for SP was 3.9 pmol/L and for CGRP and NPY it was 7.8 pmol/L. The average intra-assay CV was 10%.

CHARACTERIZATION

To characterize the immunoreactivity obtained by RIA, reverse phase high performance liquid chromatography (HPLC) was done. HPLC equipment (Gilson, Villiers-le-Bel, France) and a Waters Delta Pak (C18, 300 Å) 3.9 mm x 150 mm column were utilized.

The samples were filtered using Millipore GS filters (0.45 µm) and 200 µl of each sample was injected into the column. Samples were eluted with a 40 min linear gradient of acetonitrile in water containing 0.1% trifluoroacetic acid and fractions of 0.5 ml collected at a rate of 1.0 ml/min. A gradient of 10-60% was used for SP and CGRP, and 20-70% for NPY. The fractions were lyophilized, reconstituted in 100 µl of distilled water then assayed by RIA (Fig.4). A peak was observed indicating the fraction containing the ligand to which the RIA antibody was bound. In separate runs, control peptides (8000 pmol/L) were also analysed in the same way as the samples.

The peaks from the control peptides were found to elute in the same fractions as the samples. The elution fraction containing the main immunoreactive peak of each neuropeptide corresponded to that of the synthetic peptide, confirming the specificity of the immunodetection and the integrity of the neuropeptide of interest.

Figure 4. HPLC
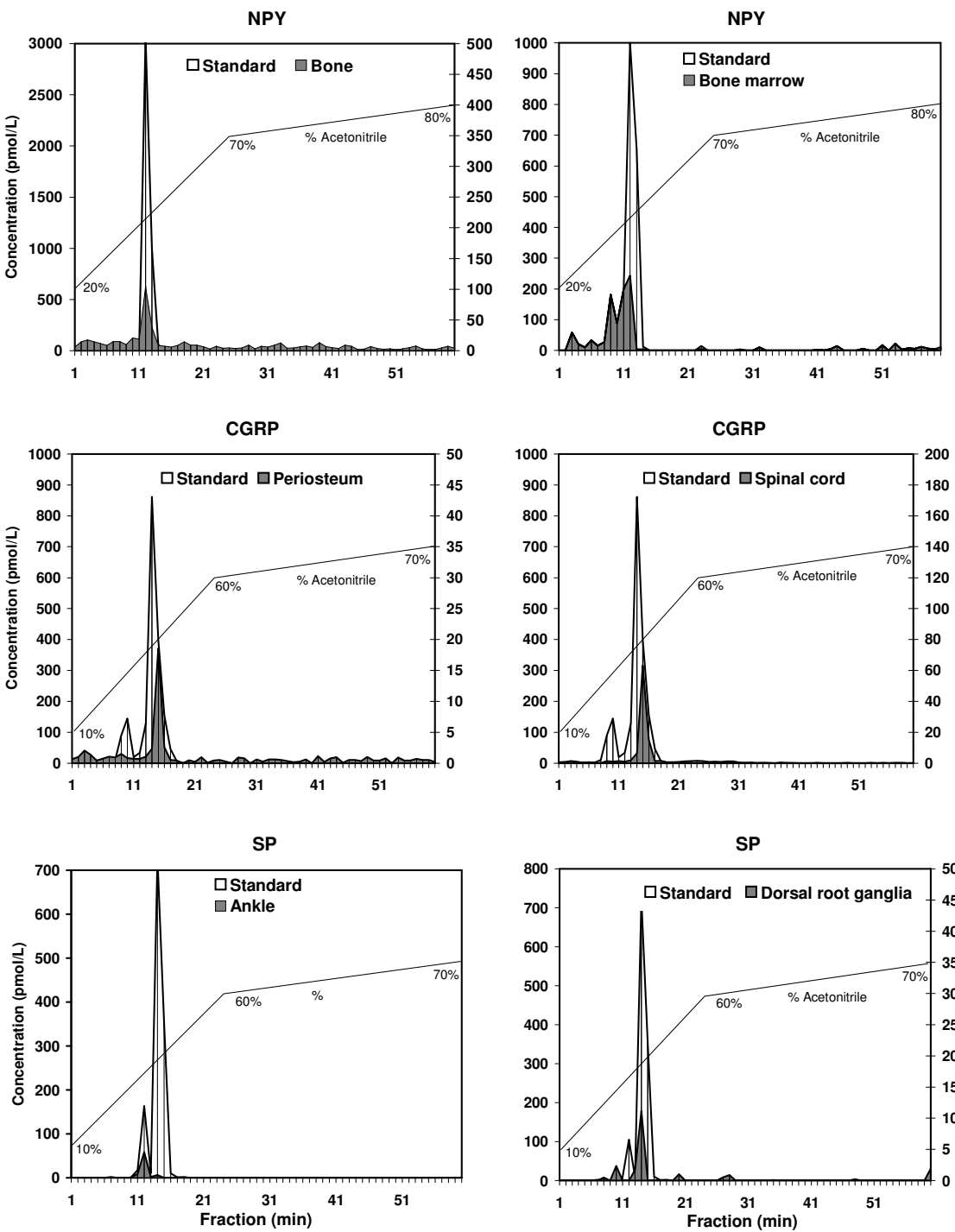
IMMUNOASSAYS – IGF-I AND IGFBPS

Quantitation of IGF-I, IGFBP-1 and IGFBP-4 and insulin in serum, and IGF-I in tissue extracts was done by immunoassays.

Serum IGF-I concentrations were determined by RIA after acid ethanol extraction and cryoprecipitation, and using truncated IGF-I as tracer, based on the method of Bang et.al.[110]. The intra- and inter-assay variation was 4% and 11%, respectively.

IGFBP-1 concentrations were measured using a plate immunoassay described in a previous study[111]. The intra- and inter-assay variation was 5% and 15%, respectively.

IGFBP-4 was measured by RIA at the laboratory of Growth and Development, California Pacific Medical Center Research Institute, San Francisco, CA, USA according to the method of Chelius et.al[112]. Serum IGFBP-4 levels in control rats from the current project have been reported by Chelsius. The intra- and inter- assay variation was 3% and 8%, respectively.

Serum insulin was measured using a commercial rat insulin RIA kit (Linco Research, St. Charles, MO, USA). The intra- and inter- assay variation was 6% and 8%, respectively.

STATISTICS

Variables were summarized according to mean and standard deviation. Parametric tests (Student's t-test and ANOVA) were used for all group comparisons except when data was skewed, whereby Mann-Whitney test was applied. Pearson's test was used for correlations. Effect of variability of body weight on the bone parameters was analysed by test of covariance (ANCOVA) and correlation. An α-level of 5 percent was chosen. Results are presented as histograms; raw data is also included in tabular form in the Appendix A. In histograms, the level of significance is indicated as *=p<0.05, **=p<0.01. ***=p<0.001.

SKELETAL FEATURES

PAPER I,II

SIZE AND FORM

In the 12-month-old diabetic rats, the length of humerus and height of vertebrae were reduced by 8%, whereas the length of tibia and metatarsal was not (Fig.5). In fact, the latter was longer though marginally (2.9%). The tibial length at 20 months was greater than at 12 months in both diabetic and control rats. GK rats are known to grow less than Wistar rats[85]. From the current results it appears that in diabetic rats, bone size is decreased only in the axial and upper limb bones, while the hind limb bones are unaffected. Since the hind- and fore-limbs face different loading forces, the difference in length may indicate a change of the normal response of the growth plate to load in diabetic rats. The data does not support an overall impairment of bone growth as the tibia and metatarsal were not shorter. Thus, diabetes results in shortening of certain bones, apparently depending on load. The greater tibial length at 20 months compared to 12 months in both diabetic and control rats should be related to both age and sex. Growth probably occurred between 12 and 20 months, since rats are known to have partially open epiphyses at 12 months[113-116]. Moreover, in Wistar rats, males grow more than females, like most other rat strains.

According to regional pQCT, the diaphysis of long bones in diabetic rats expanded (Fig.6). In fact, both the periosteal and endosteal circumferences were increased, the latter reflecting endosteal erosion. The cortical thickness at 12 months was increased in the tibia, but normal in other bones. At 20 months, it was normal in the tibia, but reduced in the metatarsal. The observed, periosteal expansion can be expected to increase mechanical strength, since the cortex is placed further away from the center of the bone[117]. This can occur even in the presence of endosteal erosion causing reduction of cortical thickness, unless the latter is very extensive[118]. Endosteal erosion and periosteal expansion are normal features of long bone diaphyses in aging humans eventually resulting in cortical thinning. In the metatarsal of diabetic rats, cortical thinning was observed at 20 months (appendix A, table 17). Thus, it appears that age-related changes in diaphyseal bone occur earlier in diabetes.

In diabetic rats, the metaphyses unlike the diaphyses showed a decrease in the cross-sectional area both in the humerus and tibia, albeit it was significant only in the latter (Fig.7). In the vertebrae, no significant difference was seen. A narrower metaphysis suggests mechanical weakness. The changes were seen in both age groups, which were also of different gender.

Altogether, the changes observed in size and form of metaphysis and diaphysis seem to be consistent features of the diabetic rat skeleton.

Figure 5. Height and length
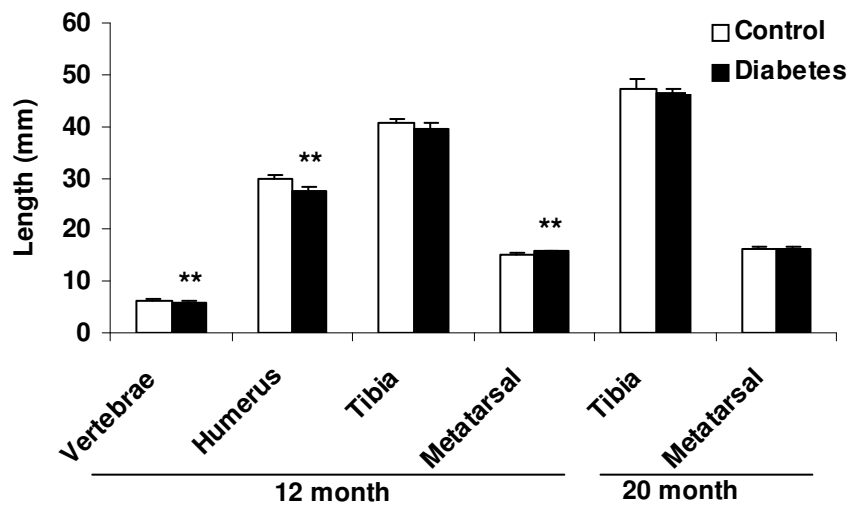
Figure 6. Circumference of diaphyses
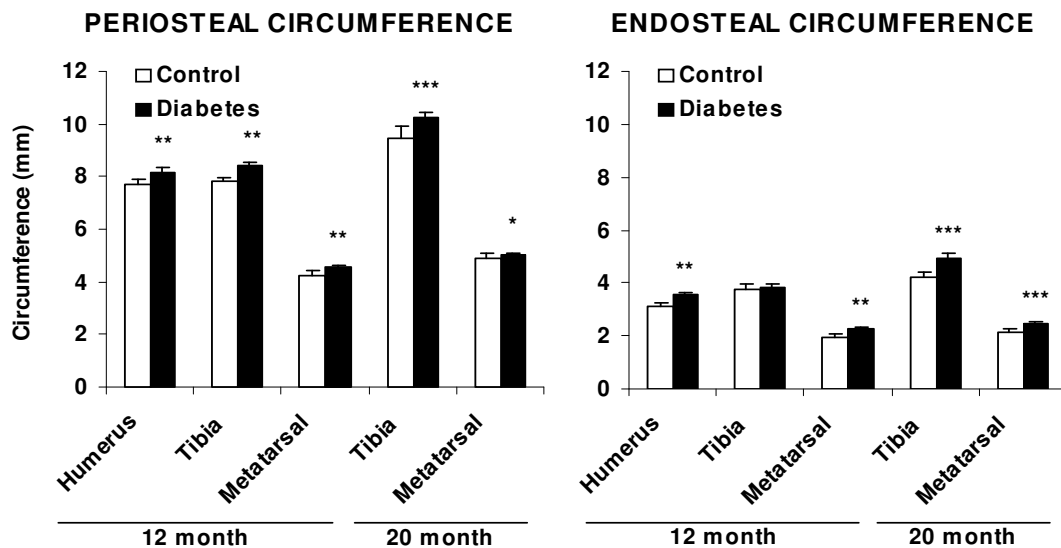
## Figure 7. Cross-sectional area – vertebrae and metaphyses
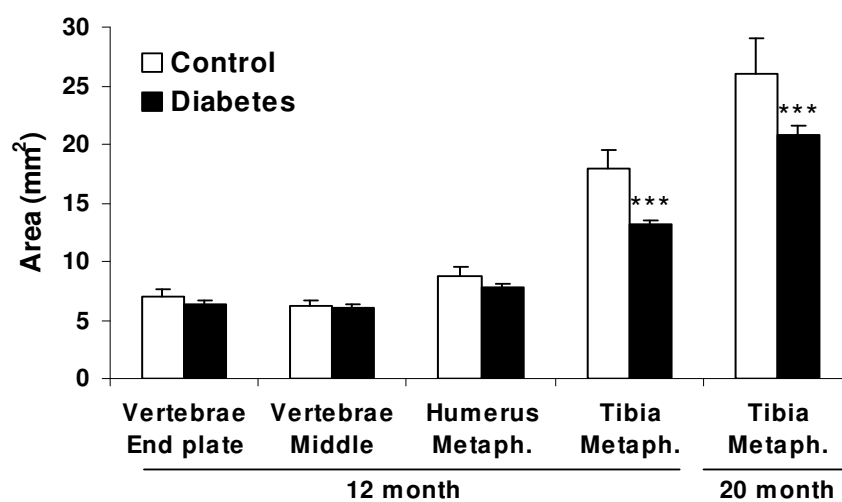
BMC

DEXA showed that whole body BMC was reduced in the diabetic rats by 9% (Fig.8). As for individual bones, a decrease was observed in all bones except the metatarsal. Since BMC is known to correlate with body weight and the diabetic rats weighed 8.7% less than controls, the lower BMC may be explained by the difference in body weight. Although the lower whole body BMC may be attributed to a smaller skeleton, a reduction in bone length was only observed in the humerus and vertebrae, not in the hind limb. Thus, the decrease in BMC despite normal length appears to indicate an absolute loss of mineral. The fact that the metatarsal did not exhibit loss of BMC should be explained by the predominantly cortical nature of the bone.

As for regional changes, the metaphysis of all long bones showed a substantial reduction in BMC (Fig.9). The diaphysis, on the other hand, showed a significant though small increase in BMC in tibia and metatarsal, but a decrease in the humerus. Most of the reduction in whole long bone BMC should be attributed to metaphyseal bone loss. The decrease in metaphyseal BMC along with an increase in diaphyseal BMC may represent a redistribution of mineral from the trabecular to the cortical portion of the diabetic rat bones. The increased BMC in diaphyseal bone presumably increases strength.

The DEXA results were corroborated by strong correlation with ash weight results (appendix A, tables 12 and 13)

BMD

According to DEXA, the areal BMD of the whole body was normal in diabetic rats. Among individual bones, a-BMD was either normal or reduced (Fig.10). The greatest reduction of a-BMD was observed in the vertebrae, the least in the metatarsals. It appears that differences in the relative distribution of the trabecular and cortical components within individual bones are responsible for the difference observed in a-BMD.

Figure 8. BMC
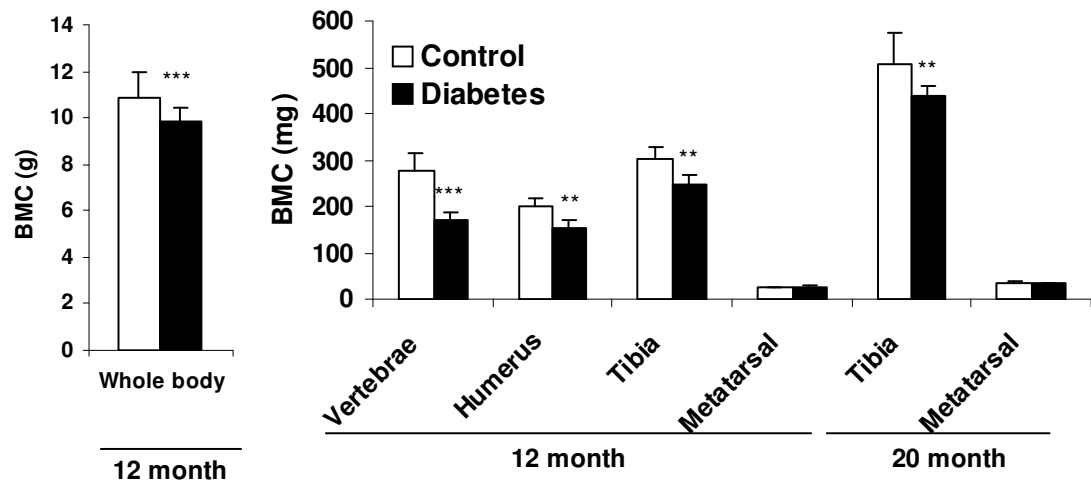
Figure 9. Regional BMC
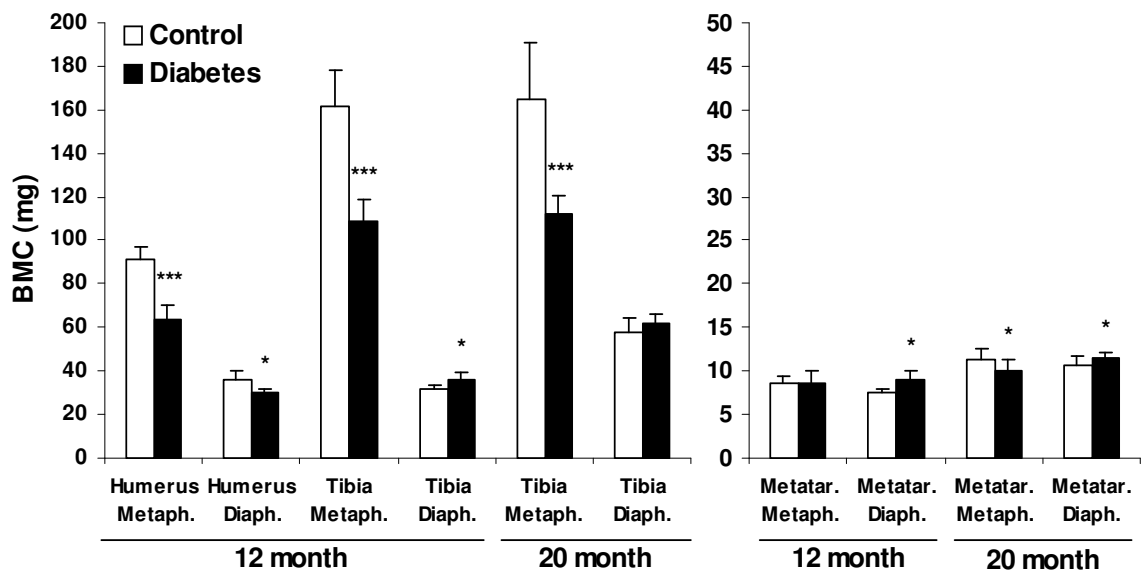


Figure 10. Areal BMD – whole bone
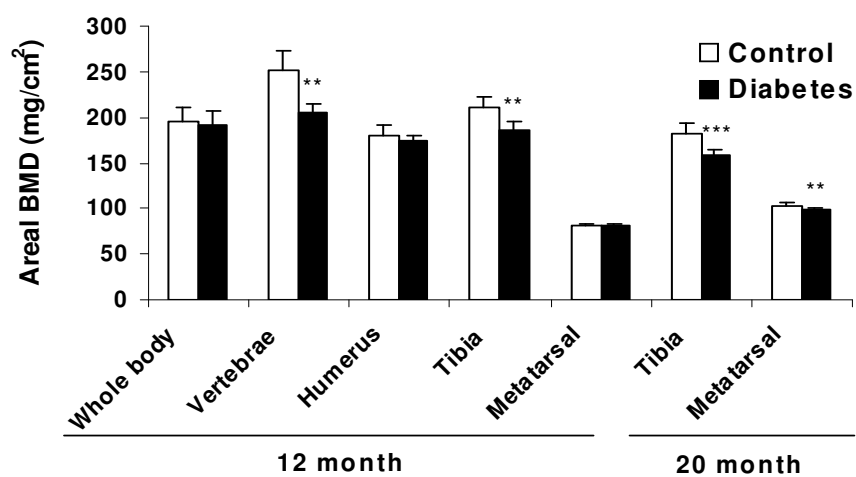
As for regional changes, there was a reduction of a-BMD in the metaphysis of tibia and humerus in the diabetic rats, while the diaphysis of all bones had normal a-BMD (Fig.11). The metatarsal showed a reduction in a-BMD in the metaphysis at 20 months, but not at 12 months. The results imply that the reduction of a-BMD predominantly pertains to sub-regions normally rich in trabecular bone. Notably, the vertebrae also exhibited reduced a-BMD, as shown before. In both diabetic and control rats, the metaphyseal and diaphyseal a-BMD of the tibia, was lower at 20 months as compared to 12 months. However, in the diabetic rats, it appears that the reduction of metaphyseal a-BMD progresses with age.

According to pQCT of cross-sections, the "true" v-BMD in diaphyseal bone was only reduced in humerus (Fig.12). In the tibia and metatarsal, there was no significant difference, which applied to both age groups. The lower v-BMD in humerus in diabetic rats may be explained by the fact that it bears less load than the other bones. It is conceivable that bone turn-over in response to loading forces is altered in diabetes. In the hind limb bones, which bear more load, the v-BMD was normal in diabetic rats. In both the diabetic and control rats, v-BMD in humerus was higher compared to tibia and metatarsal, which may be a normal feature of the rat skeleton.

In regions normally rich in trabecular bone, i.e. the metaphyses of long bones and the vertebrae, there was a substantial reduction of v-BMD (Fig.13). The total v-BMD of the cross-sections, representing an average from cortical, sub-cortical and trabecular bone, was significantly reduced (range –13 to –24%) in all bones except tibia, where a tendency (p=0.065) to lower (–10%) v-BMD was noted. Analysis of the trabecular compartments showed lower v-BMD in all bones, ranging from –33 to –62%.

The pQCT software is not able to separately provide cortical v-BMD in these regions, though trabecular v-BMD can be obtained. The decrease in trabecular v-BMD was proportionately greater than that in the total v-BMD of the cross-section. This implies that most of the reduction of v-BMD observed in these regions should be ascribed to trabecular bone.

Figure 11. Regional areal BMD
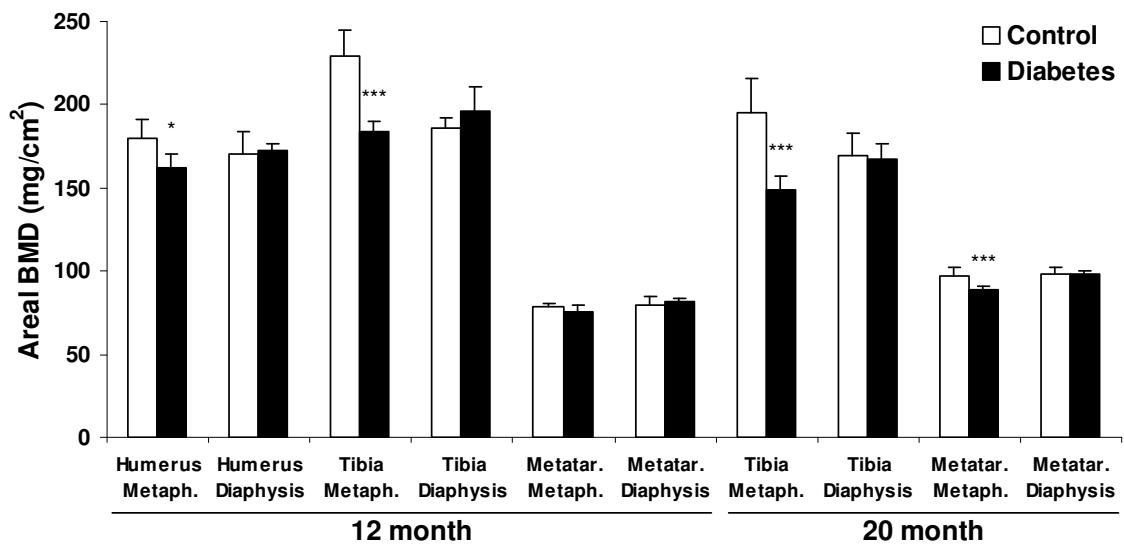
Figure 12. Volumetric BMD – Diaphysis
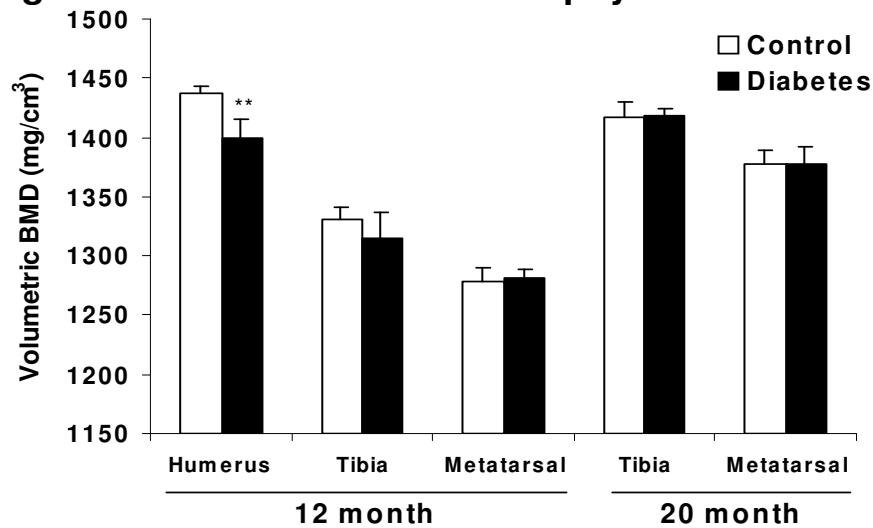
Figure 13. Volumetric BMD – Vertebrae and metaphysis
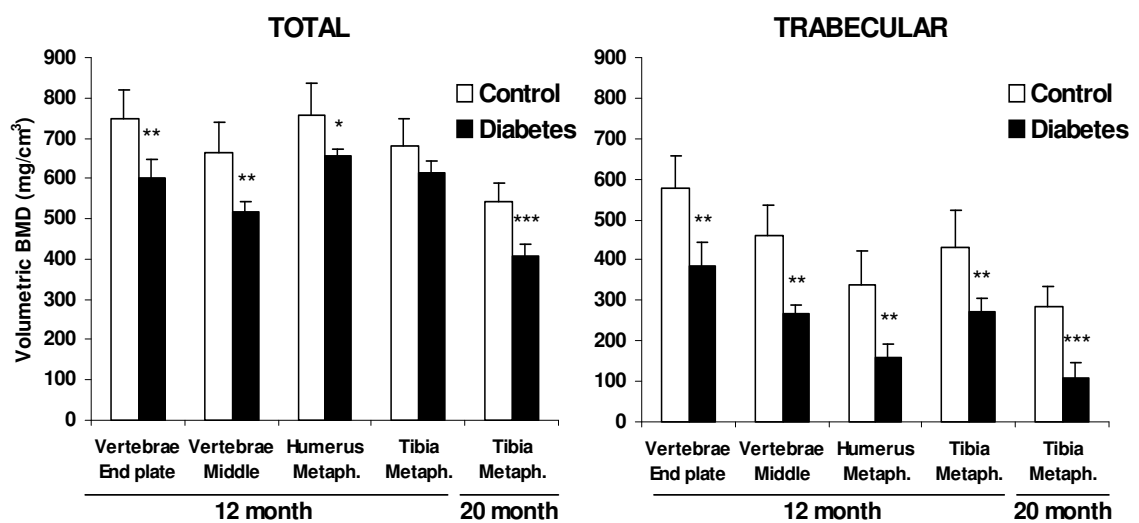
Ash density Determination of percent ash was done to assess the proportion of mineral per weight of bone. The analysis showed that there was no change in humerus and vertebrae, while in the tibia a substantial reduction of percent ash was observed in the diabetic rats, most pronounced in the metaphysis (Fig.14). The reduction was greater in the 20-month-old diabetic rats.

The finding that there was no reduction in ash density in humeral metaphysis and vertebrae seemingly contradicts the reduced BMD assessed by DEXA and pQCT in these bones. The discrepancy can be explained by the methodology. A lower a-BMD and v-BMD would be seen if there was an absolute decrease of the number of bone trabeculae. However, percent ash should be normal as long as the mineral density within the trabeculae is normal. On the other hand, a reduction in mineral density within the trabeculae should lower the percent ash. Thus, in humerus the decrease of BMD probably reflects a decrease in the number of trabeculae while in tibia, a decrease of both number of trabeculae and their mineral density.

STRENGTH

The estimate of diaphyseal strength obtained from pQCT data, i.e. the cross-sectional moment of inertia, showed an increase in all long bones in the diabetic rats, suggesting a greater bending strength (Fig 15). The moment of inertia is highly dependent on the periosteal diameter and the cortical thickness. Thus, the greater moment of inertia should be attributed to the diaphyseal expansion in diabetic rats. Notably, this index is based on cortical dimensions and does not take into account bone matrix properties, microstructure, BMC or BMD. As the volumetric BMD in diaphyseal bones was nearly normal and the BMC was increased, the increased moment of inertia probably represents a true increase in strength. However, for the bone as a whole this may well be offset by a decrease in strength because of osteopenia and narrowing of the metaphysis. Conceivably, periosteal expansion reflects an attempt to regain bone strength lost by endosteal erosion of the diaphysis and also osteopenia and narrowing of the metaphysis. The latter is supported by the apparent "redistribution" of BMC from the metaphysis to the diaphysis, as suggested before. Notably, diaphyseal fracture is not a typical feature of diabetes[119] as opposed to periarticular fractures and Charcot arthropathy[52], which may be explained by the metaphyseal loss of trabecular bone.
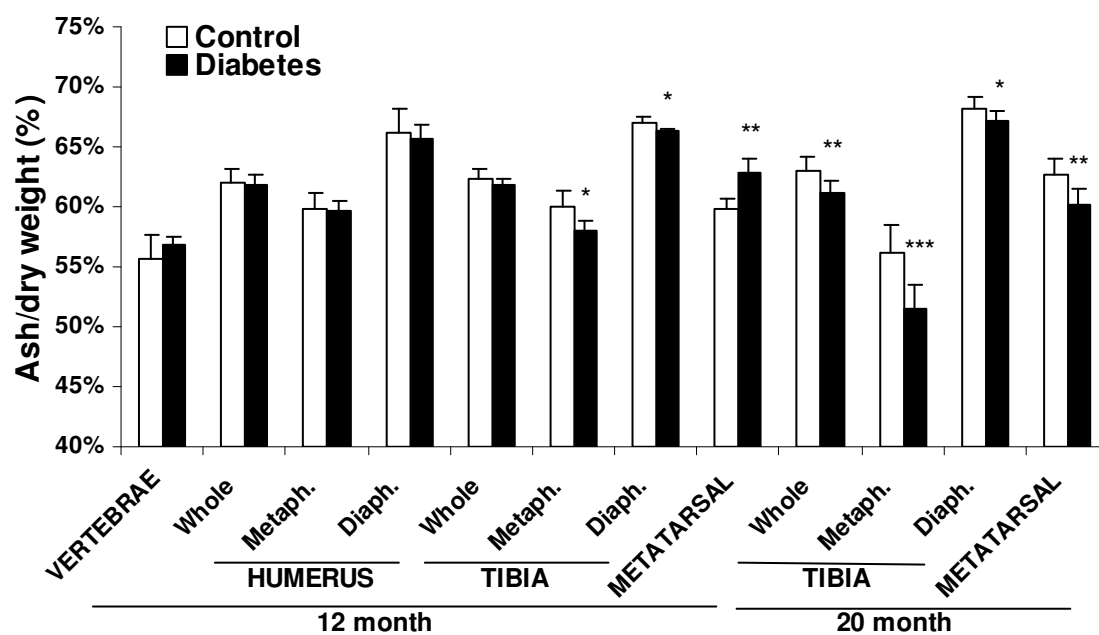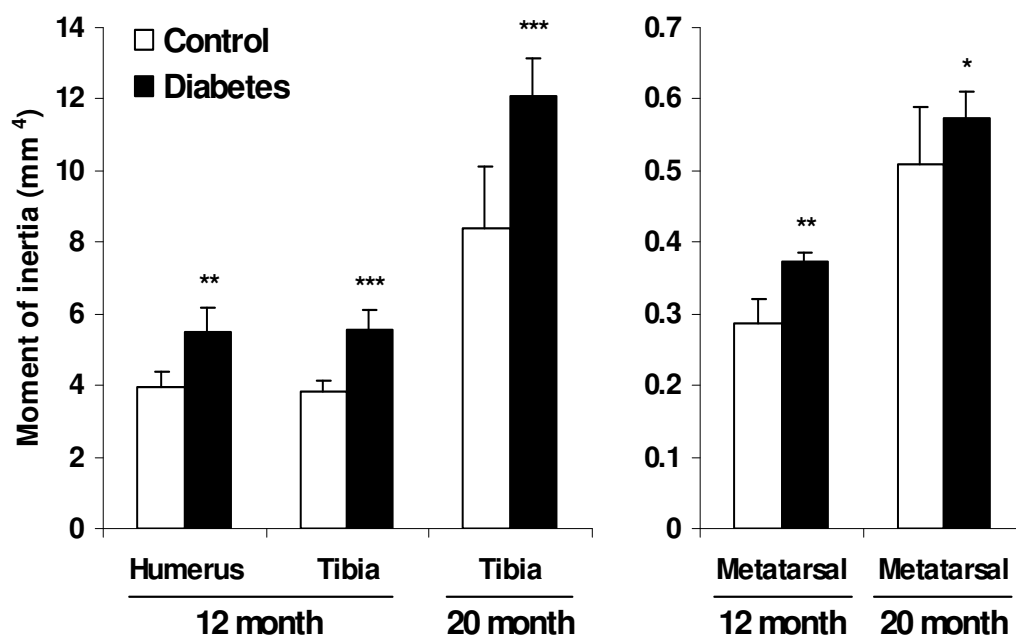
Figure 14. Percent ash

Figure 15. Cross-sectional moment of inertia

COMMENTS

The above data shows that the typical features of the diabetic rat skeleton are trabecular osteopenia in vertebrae and long bones metaphyses, and also endosteal erosion and periosteal expansion of diaphyses. The literature suggests that metaphyseal osteopenia is also a typical feature of human diabetes. Thus, metaphyseal fractures of the proximal humerus have been noted to occur more frequently in the diabetic population even after correction for age, body mass index and differences in BMD[7]. Recently, a multi-center study of patients sustaining distal radius fractures[6] reported that the risk of intra-articular fracture was increased two-fold in diabetics, but not that of extra-articular fractures. A pQCT study examining metaphyseal bone in diabetic patients demonstrated a significant reduction of trabecular BMD (Z-score) of the distal radius[120]. Presumably, the clinical implication is greater risk of metaphyseal, juxta-articular and intra-articular fractures in diabetes. These reports support our findings, and reinforce the notion that the bone weakness in diabetes pertains not to the diaphyses of long bones, but to the regions normally rich in trabecular bone. Osteopenia has been suggested as one of the factors behind the development of Charcot joint[10,121]. Trabecular osteopenia in the metaphysis presumably predisposes to subchondral bone collapse. Notably, increased levels of markers of osteoclastic bone resorption have been found in Charcot arthropathy[122].

In a previous study on the femur in streptozotocin-induced type-1 diabetic rats, a significant reduction of bone growth was noted along with metaphyseal osteopenia. Interestingly, diaphyseal BMD was greater than "expected" considering the decreased bone growth. However, the study utilised single-photon absorptiometry and no assessment of diaphyseal dimensions was done. Thus, the higher BMD may well have been due to diaphyseal expansion, considering the results of the present study.

The regional differences in bone dimensions and mineral content prompt a reassessment of the methodology to be used for detection of diabetic osteopathy. If the v-BMD of two bones is equal, their a-BMD may not be equal if their outer dimensions are different[24]. Notably, conventional scanning protocols for DEXA do not consider variations in bone dimensions while calculating BMD. In a recent editorial[123] on fractures in diabetes it was stated that *"…a normal bone mass, as conventionally assessed by DXA and related modalities, can be offset by bone fragility at certain fracture sites and the likelihood of injury to these sites."* DEXA, the most commonly used method for bone mineral evaluation, cannot adequately determine trabecular osteopenia, nor cortical expansion. Thus, pQCT may be the method of choice for the assessment of diabetic osteopathy.

It may be questioned whether the changes observed in the humerus and vertebrae are due to decreased bone size and/or the difference in body weight. However, no correlation was found between bone length on one hand, and v-BMD and cortical dimensions on the other. Moreover, the changes remained significant despite correction for differences in bone length and body weight according to analysis of covariance (data not shown). Furthermore, the magnitude of the decrease in the trabecular v-BMD was much greater than the reduction in length. Trabecular osteopenia is unlikely to be due to a smaller bone because v-BMD is not affected by differences in bone size. This is one of the main advantages of BMD assessments by QCT as compared to DEXA[24]. As for cortical dimensions, a reduction of length should be accompanied by a reduction in the periosteal circumference, but the opposite was observed in the diabetic rats.

Our data shows that bone changes in diabetic rats are specific to bone and sub-region. This implies that local factors may be more important than systemic calcium regulating hormones in the pathogenesis of diabetic osteopathy. A variety of local factors are known to regulate local bone turn-over[124], including prostaglandins, cytokines, growth factors and neuropeptides. Given the skeletal findings in diabetic rats with neuropathy, the subsequent investigations focused on the insulin-like growth factor (IGF) system and sensory as well as autonomic neuropeptides in bone and joints.

IGF SYSTEM

PAPER III

Analysis of insulin, IGF-I and IGFBPs in 12-month-old diabetic and control rats was done in serum, while IGF-I was also analysed in samples from ankles and cortical bone.

SERUM

Serum insulin levels in the diabetic rats were not significantly different from controls though it tended to be lower (Table 3). However, serum IGF-I levels were clearly lower in diabetic rats, while IGFBP-1 and -4 levels were significantly higher. IGF-I is known to be a trophic factor for bone. A deficit may indicate a causal link to osteopenia. The increased levels of IGFBP-1 and -4 are expected to decrease circulating IGF-I bioavailability and thereby decrease the trophic effect of IGF-I on bone.

BONE AND JOINT

In diabetic rats a significant reduction of IGF-I was found in cortical bone, but not in ankles (Fig.16). The levels presumably reflect both endocrine as well as paracrine IGF-I. Regardless of the source, these local levels can be expected to have significance for local bone turnover. In diabetic rats, the local IGF-I deficiency in cortical bone presumably underlies the endosteal erosion observed in the diaphysis, although compensated by periosteal bone formation.

Table 3. Serum insulin, IGF-I and IGFBP levels (mean ng/ml ± SEM).

	Control	Diabetes	Difference (p-value)
Insulin	1.6 ± 0.5	1.1 ± 0.3	-30.7% (0.463)[a]
IGF-I	205 ± 50	168 ± 26	-18.0% *(0.009)*[b]
IGFBP-1	21 ± 5	39 ± 32	89.2% *(<0.001)*[a]
IGFBP-4	422 ± 53	505 ± 71	19.7% *(<0.001)*[b]

a,b: p-value according to Mann-Whitney U test (a) and T-test (b).

Figure 16. Bone and joint IGF-I. Error bars=SEM
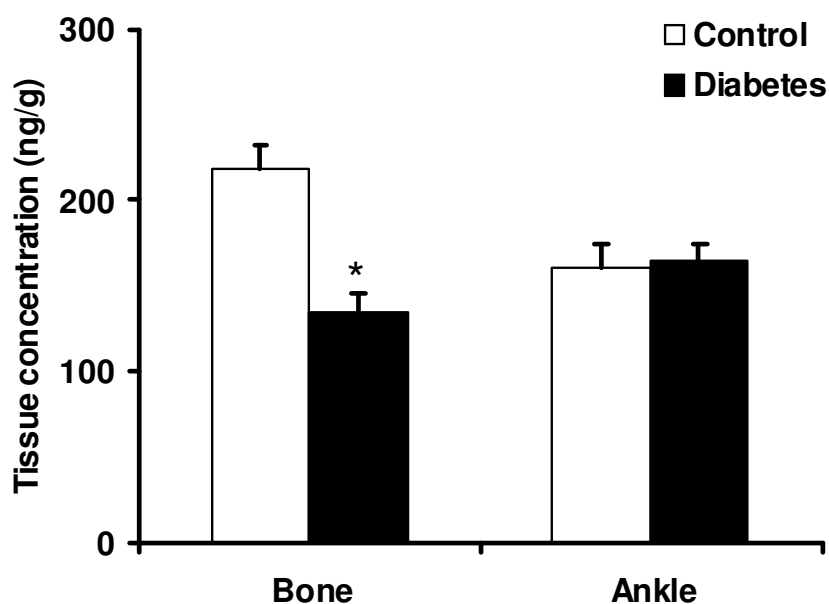
COMMENTS

The results show that the IGF system in diabetic rats with regional osteopathy is disturbed not only systemically, but also locally. It may prove that the skeletal features demonstrated in diabetic rats are related to this disturbance. In insulin deficiency of human type-1 diabetes, serum IGF-I is decreased, while IGFBP-1 is increased. These observations are in line with the results of the current study. Moreover, the lower IGF-I and higher IGFBPs in the serum in the diabetic rats comply with lower whole body BMC, also with lower metaphyseal BMC and BMD, as would be expected from reduced IGF-I activity. In cortical bone, the IGF-I level may be assumed to reflect both endocrine and paracrine IGF-I. The decrease observed implies that the anabolic effect of IGF-I on bone cells is reduced.

The diaphyseal findings in diabetic rats may appear to speak against the probable effect of decreased systemic and local IGF-I levels considering the expansion of the humeral and tibial diaphyses. However, the main effect of IGF deficit is probably endosteal erosion, eliciting a compensatory

periosteal expansion in response to load. The metaphyseal decrease in BMC, presumably caused by low IGF-I, and the concomitant increase in diaphyseal BMC possibly reflect a redistribution of mineral. Given that both systemic and local IGF-I deficit in diabetes leads to bone loss, it appears that the response to this loss decisively differs between trabecular and cortical bone. While cortical bone responds to the endosteal erosion by periosteal bone formation, trabecular bone in the metaphyses does not seem to have this compensatory mechanism. It may prove that the adverse effect of the disturbed IGF-system in diabetes is confined to the inner surfaces of bone, whereas the outer escape from major loss by compensatory mechanisms. In the elderly population, metaphyseal osteopenia and cortical expansion are also seen[26] concomitantly with a decline in serum IGF-I levels. Thus, the bone changes observed in the diabetic rats seem to mimic early bone aging.

Considering that in diabetic rats, IGF-I levels were reduced in both serum and cortical bone, it was unexpected to find normal IGF-I level in ankles. Possibly, this can be explained by a high contribution of local IGF-I levels in non-osseous tissues of the ankle, such as cartilage, synovium, ligaments, tendons, surrounding blood vessels and areolar tissue.

As for the higher IGFBP-1 and -4 levels in diabetic rats, they comply with decreased BMD, since both have an inhibitory effect on IGF-I activity and hence, bone formation. However, systemically administered IGFBP-4 has been shown to have direct bone formative effects *in-vivo* unlike its *in-vitro* effects[125]. The *in vivo* effect has been attributed to proteolytic fragments of this protein. The predominant role of paracrine IGFBP-4, however, is one of sequestration of IGF-I and inhibition of the latter's action[126]. The results of the current study suggest that in diabetic rats, the relation between local IGF-I levels and BMD is altered. To what extent IGFBP-1 and -4 levels influence this relationship is unclear. Other IGFBPs may also be of significance, especially IGFBP-5, which has been reported to act as a growth factor for bone[44].

In diabetic rats, relative insulin deficiency, hyperglycemia and altered IGFBP activity may affect the relation between IGF-I and BMD. Although serum insulin levels in our diabetic rats were not significantly different

from controls, previous studies on the GK rats have shown higher insulin levels in early life and lower levels in older age, as compared to age- and sex-matched control rats[85,87]. However, at all ages they exhibit a blunted insulin response to glucose challenge, and thus have a relative insulin deficiency. This deficiency may well contribute to decreased BMD considering that insulin is a growth factor for bone.

It may be concluded that this is the first study demonstrating abnormalities of the IGF-system in rats with type-2 diabetes and regional osteopathy. It is also the first study on local IGF-I levels in bone. From the results, it appears that not only the systemic levels of IGF-I are related to the observed bone changes, but also the local levels. However, regional osteopathy in diabetes cannot be exclusively explained by IGF-I. Apart from its interactions with IGFBPs, and the direct effects of the latter on bone, there are other local factors of importance for local bone turn over. In addition to different factors acting independently of the IGF system in bone, it may prove that the diabetic complications related to IGF system abnormalities, such as neuropathy[127], also contribute to the development of diabetic osteopathy.

NEUROPEPTIDES

PAPER IV

In 12-month-old diabetic and control rats the occurrence of sensory and autonomic neuropeptides in bone and joint as well as spinal cord and dorsal root ganglia was assessed by immunohistochemistry and RIA.

MORPHOLOGY

In both diabetic and control rats, immunohistochemical analysis showed the presence of sensory (SP, CGRP) and autonomic (NPY) nerve fibers in bone and joints (Fig. 17A-D), although in general they were quite sparse. An abundance of perivascular nerve fibers, both sensory and autonomic, was seen in the loose connective tissue, synovium and cortical bone, while non-vascular nerves were frequently seen in the periosteum and bone marrow.

Figure 17 A-D.
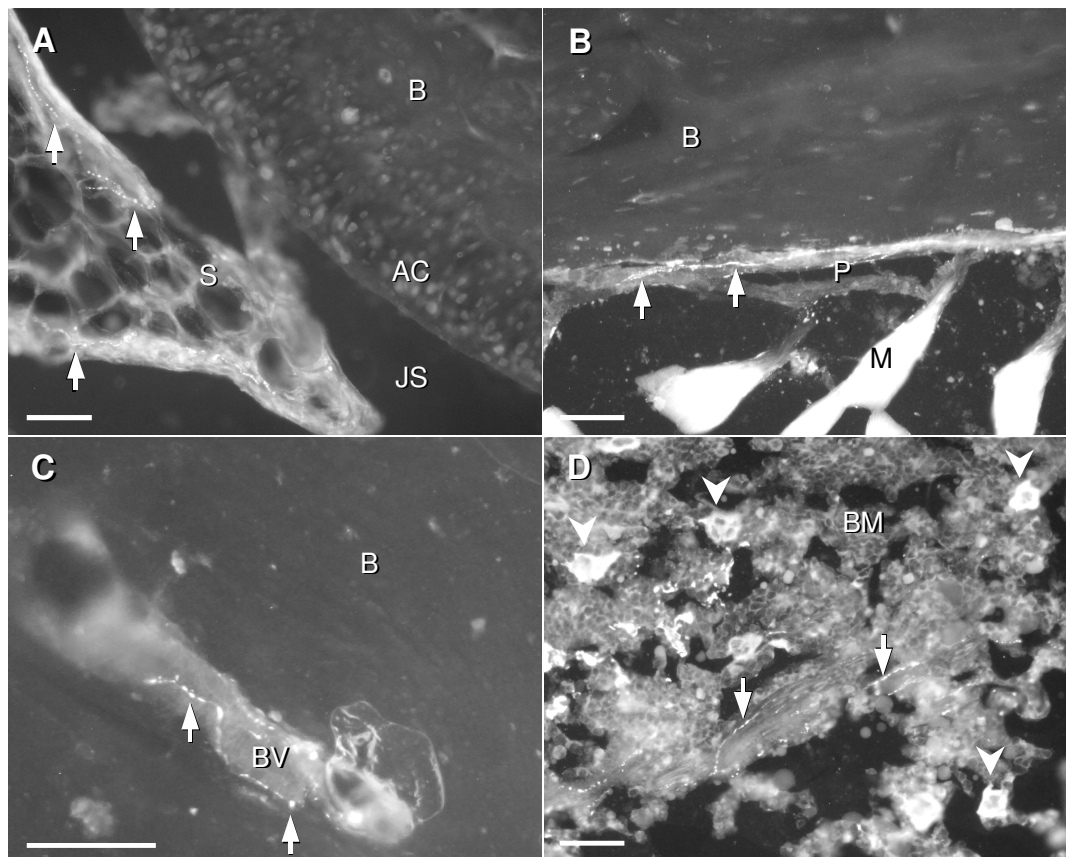
Photomicrograph of sections through bone and jonts stained immunohistochemically for SP (A), CGRP (B) and NPY (C,D). Nerve fibers (arrows) positive for SP in synovium (A) and CGRP in periosteum (B) are shown. NPY-positive nerve fibers (C) are seen in a vascular channel in cortical bone. In bone marrow in tibial diaphysis (D), NPY-positive nerve fibers (arrows) and cells (arrow-heads) are observed. S=synovium, AC=articular cartilage, JS=joint space, B=bone, P=periosteum, M=muscle, BV=blood vessel, BM=bone marrow. Bar=50µ.

As for the distribution of sensory versus autonomic nerves, there were, certain differences. Thus, in the bone marrow, SP and CGRP fibers were only occasionally seen, and were mostly peri-vascular, while NPY-nerve fibers were frequently observed both vessel related and as free nerve terminals. Notably, cellular immunoreactivity to NPY was also observed in large multinucleated megakaryocytes and occasional mononuclear hematopoietic cells of the bone marrow. In cortical bone, NPY-nerves were seen in vascular canals, more frequently near the endosteal surface. In addition to bone and joints, the occurrence of SP and CGRP was also analysed in dorsal root ganglia and the spinal cord. As expected, immunoreactivity for both neuropeptides in GK rats as well as controls was found in lamina I and II of the dorsal horn and the cell bodies of the dorsal root ganglia. Over all, the immunoreactivities of the tissues analysed, besides bone marrow, were confined to neuronal structures, but no clear difference between diabetic rats and controls could be seen.

TISSUE LEVELS

RIA for SP and CGRP in bone and joints showed no significant differences between diabetic and control rats, although the mean values suggested an increase in CGRP and a decrease in SP (Table 4). The results for SP in periosteum and bone marrow were excluded because the values were below or near the detection limit ($\downarrow$).

Table 4. Tissue neuropeptide levels according to RIA (pmol/g wet weight)

	Control (n=21)	Diabetes (n=18)	Difference (p-value)
SP			
Bone	0.14 ± 0.11	0.08 ± 0.05	-40.4% (0.255)
Periosteum	$\downarrow$	$\downarrow$	
Bone marrow	$\downarrow$	$\downarrow$	
Ankle	0.20 ± 0.17	0.21 ± 0.19	7.3% (0.694)
Dorsal root ganglia	0.74 ± 0.17	0.68 ± 0.15	-7.9% (0.346)
Spinal cord	19.2 ± 5.33	19.92 ± 5.44	3.7% (0.732)
CGRP			
Bone	0.24 ± 0.11	0.30 ± 0.12	22.0% (0.243)
Periosteum	0.21 ± 0.07	0.26 ± 0.08	19.8% (0.311)
Bone marrow	1.64 ± 1.20	1.21 ± 0.95	-26.3% (0.132)
Ankle	1.24 ± 0.28	1.40 ± 0.38	13.2% (0.194)
Dorsal root ganglia	24.09 ± 5.64	17.80 ± 4.19	-26.1% *(0.002)*
Spinal cord	87.06 ± 15.79	70.48 ± 15.57	-19.0% *(0.010)*
NPY			
Bone	3.65 ± 0.88	2.33 ± 0.57	-36.2% *(<0.001)*
Periosteum	1.49 ± 0.87	1.07 ± 0.54	-28.5% (0.156)
Bone marrow	92.9 ± 46.1	31.22 ± 17.60	-66.4% *(<0.001)*
Ankle	1.05 ± 0.38	0.75 ± 0.21	-28.7% *(0.016)*
Spinal cord	42.01 ± 15.33	43.04 ± 9.11	2.4% (0.835)

The concentration of NPY in bone and joints was significantly decreased in diabetic rats (Table 4), in cortical bone by 36%, in bone marrow by 66% and in ankle by 29%. In the spinal cord and dorsal root ganglia, CGRP, but not SP, was significantly lower (19%, 26% respectively).

COMMENTS

From the results it is obvious that diabetic rats exhibit distinct peripheral neuropeptidergic changes in bone and joints. The most conspicuous findings pertained to the autonomic peptide NPY, which was substantially reduced in these tissues, while the sensory peptide CGRP was reduced in the spinal cord and dorsal root ganglia. In diabetic rats neuropathy has previously been described in terms of reduced nerve conduction velocity and morphological changes of the nerves, and lately, also in terms of neuropeptidergic changes in peripheral tissues such as the dorsal root ganglia, sciatic nerve and skin[80-82]. The present study, however, is the first report on neuropeptide occurrence in bone and joints in diabetes. The changes observed may prove to contribute to the development of diabetic osteopathy.

Among sensory neuropeptides, SP has been found to be a potent bone resorptive factor[62,63] and its receptor (NK-1) has been demonstrated in osteoblasts, osteocytes and osteoclasts[67] CGRP inhibits bone resorption[64] suppresses osteoclastogenesis[65] and increases osteoblast proliferation[66]. In this study, a decrease in CGRP was seen in the DRG and spinal cord, whereas in bone and joints the changes were insignificant. Considering the mild form of diabetes in these rats, the sensory neuropathy may not yet be advanced enough to involve bone and joint tissue. If, at a later stage the deficit of CGRP propagates to bone and joints, it would likely result in enhanced bone resorption, given the known anti-resorptive effect of CGRP.

From our study, it appears that autonomic neuropathy is more pronounced than sensory. This complies with observations on diabetic patients, in which the onset of sub-clinical autonomic nerve dysfunction precedes that of sensory dysfunction[128,129]. Notably, a decrease of NPY but not of CGRP or SP, has been reported in a clinical study on forearm skin in diabetes patients[130]. The greatest deficit of NPY was found in the bone marrow. Since immunohistochemistry showed that several cell types in the bone marrow stained positive for NPY, the deficit according to RIA may reflect partly cellular loss and partly neuronal. However, in cortical bone and ankles staining was confined to nerve fibers. Thus, the loss in these tissues of NPY should be ascribed to neuronal tissue.

NPY is produced in the peripheral nervous system in sympathetic ganglia and is co-released with noradrenaline from sympathetic nerves. It has a sustained vasoconstrictory effect, confirmed also in bone[129]. Diabetic patients with autonomic neuropathy exhibit abnormalities of vasoregulation[48]. Moreover, increased bone resorption[50,51] has been noted in the presence of abnormal vasoregulation. In the current study, most of the NPY-nerve fibers in cortical bone were seen in the Volkmann's canal, alongside blood vessels. Moreover, most of the nerve fibers in the bone marrow were perivascular. The loss of NPY is therefore likely to disturb normal vasoregulation and thus promote bone resorption.

Among autonomic neuropeptides, vasoactive intestinal polypeptide (VIP) has been shown to act on both osteoclasts as well as osteoblasts[70,132]. In this study, however, the focus was on NPY, which also has effects on bone turn-over through a variety of central and peripheral mechanisms. In the central nervous system, NPY acts as a downstream mediator of leptin, and thus exerts an anti-osteogenic effect[133]. In the periphery, sympathectomy by surgical[73] or chemical[74] methods, presumably reducing NPY levels, has been shown to increase osteoclast number and surface. Although the opposite has been reported by Cherruau et.al[134], there are other reports supporting an anabolic effect of NPY on bone. NPY attenuates the effect of noradrenaline on osteoblasts[69]. Since blockage of noradrenaline action by receptor antagonist results in an increase of bone mass[133], it is likely that attenuation of noradrenaline action by NPY results in a pro-osteogenic or anti-resorptive effect on bone. Indirect evidence of the presence of NPY receptors on osteoblasts *in-vitro* has been reported[69].

Although specific causal mechanisms have not been elucidated in the present study, it is likely that decreased occurrence of NPY in bone and joints contributes to the development of diabetic osteopathy.

SUMMARY AND CONCLUSIONS

The present study on non-obese Goto-Kakizaki (GK) rats with type-2 diabetes and neuropathy was an attempt to describe and define pertinent features of diabetic osteopathy. Altogether, the study included 33 diabetic GK-rats aged 12 and 20 months, and 36 age-matched Wistar rats as controls. All underwent test of glucose tolerance and nerve (sciatic) conduction velocity (NCV) showing that the diabetic rats had significantly higher blood glucose levels and lower NCV, confirming the presence of diabetes and neuropathy.

Radiologic analysis showed regional changes of the diabetic skeleton. Thus, the length of humerus and height of vertebrae was reduced and the long bones exhibited both endosteal erosion and periosteal expansion of the diaphyses. Bone mineral content (BMC) of the whole skeleton according to DEXA was significantly reduced mainly because of loss in the vertebrae and metaphyses of long bones. The latter regions also showed a significant decrease in areal bone mineral density (a-BMD), whereas no such decrease was seen in the diaphyses. Cross-sectional measurements by pQCT permitting determination of volumetric (v-) BMD and separation of cortical and trabecular bone showed that the decrease in v-BMD almost exclusively pertained to trabecular bone (vertebrae, metaphyses), whereas v-BMD of the cortical bone of diaphyses was only marginally affected.

The results indicate that juxta-articular trabecular bone in diabetes is substantially weaker, whereas diaphyseal cortical bone may be even stronger. Thus, the diaphyseal expansion increased the cross-sectional moment of inertia, an estimate of bending strength, in the diabetic rats. Admittedly, this is only a calculated index based on cortical dimensions and does not take into consideration bone microstructure, BMC or BMD. However, since the volumetric BMD in diaphyseal bones was nearly normal and the BMC was increased, the increased moment of inertia probably represents a true increase in strength. Notably, virtually all reports on the increased risk of fracture in diabetic patients deal with juxta-articular fractures, not diaphyseal fractures.

In the diabetic patient population, a screening of different bones by pQCT may identify the typical bone and sub-region having the most pronounced osteopenia as compared to controls. Routine pQCT of such a defined site may enable detection of early diabetic osteopathy. This could be used to establish the indication for preventive treatment to reduce the risk of fracture and development of Charcot joint. The approach may also be applied to diabetic patients having sustained a fracture to detect the

subset at increased risk of developing post-traumatic osteopenia and/or Charcot joint.

From the present study, it is not possible to establish whether the skeletal changes in the diabetic rats are due to the metabolic disorder or genetic differences between the diabetic and Wistar rats. Since the diabetic rats are bred from Wistar rats, they are expected by virtue of the breeding procedure to be genetically more similar to the Wistar than any other strain. The type-2 diabetes in the GK-rat is likely to be polygenetic, similar to human type-2 diabetes. This implies that a diabetic rat cannot be genetically identical to a non-diabetic rat. Quite possibly, the genes responsible for the diabetic disorder may also affect bone. Nonetheless, it remains that the observations made in the diabetic rats reflect that the diabetic skeleton is characterized by regional changes in size, form, mineral content and density, and mechanical properties, which cannot be exclusively explained by systemic factors like calcium regulating hormones. Local bone turn-over is regulated by complex mechanisms involving cytokines, prostaglandins, growth factors and, notably, also neuropeptides. Given the focus in the present study on osteopathy in diabetes complicated by neuropathy, further analysis aimed at exploring the insulin-like growth factor (IGF)-system and neuronal mediators in bone.

Immunoassays of IGF-I were done on serum, ankle samples and cortical preparations from femur and tibia. In addition, IGFBP-1 and -4 were analysed in serum. In diabetic rats, serum IGF-I was significantly reduced, whereas IGFBP-1 and -4, known to inhibit IGF-I actions, were significantly increased. These may underlie the metaphyseal osteopenia. In cortical bone, IGF-I was also significantly reduced. Thus, there was both a systemic and local reduction of IGF-I bioavailability. In cortical bone, the loss of IGF-I in diabetes represents a novel finding. Given the cortical expansion observed in diabetic rats, an increase in IGF-I would be expected. Conceivably, loss of IGF-I causes endosteal erosion which, however, is compensated by periosteal expansion in response to load. Our data suggests that the response to IGF deficit depends on the type of bone, i.e. cortical or trabecular. In the former, the endosteal erosion is compensated by periosteal expansion, maintaining cortical thickness. However, in trabecular bone, there is no such compensatory mechanism, hence an absolute osteopenia results.

The investigation of bone and joint neuropathy entailed immunohistochemistry of neuropeptides applied to ankles and tibial diaphyses, and RIA for separate preparations of periosteum, cortex and bone marrow from femur and tibia and whole ankles, in addition also

dorsal root ganglia (DRG) and lumbar spinal cord. The analyses focused on two sensory mediators, i.e. substance P (SP) and calcitonin gene-related peptide (CGRP), and one autonomic, i.e. neuropeptide Y (NPY). The morphological analysis showed that most immunopositive fibers were vessel related, although free terminals in bone and synovia were also observed without any discernible difference between diabetic rats and controls. A conspicuous finding was the abundance of NPY-positive megakaryocytes and mononuclear cells in bone marrow. RIA revealed a significant decrease of CGRP, albeit not SP, in DRG and spinal cord in the diabetic rats. As for bone, only NPY was significantly reduced, most evidently in bone marrow, but also in cortical bone and ankles. Given the bone anabolic effects of NPY and CGRP, the deficit of these neuropeptides may prove, at least partly, to underlie the loss of bone observed in diabetic rats. From our study, it seems that autonomic neuropathy is more pronounced than sensory in diabetic rats with mild to moderate diabetes, representing an early stage of the disease.

Our combined findings suggest that osteopathic changes in diabetes are related to abnormalities of the IGF system and peripheral neuropeptide occurrence. However, the exact causal relationship and the specific mechanisms involved have yet to be elucidated.

In summary, this is the first study to show that the skeleton of diabetic rats with type-2 diabetes and neuropathy is characterized by regional structural changes and abnormalities of IGF and neuropeptides, suggesting that also local factors beyond systemic play a role in the development of diabetic osteopathy.

ACKNOWLEDGEMENTS

First and foremost, I thank with all sincerity the One who introduces Himself as:

"... He has made subservient to you whatsoever is in the heavens and whatsoever is in the earth, all, from Himself; most surely there are signs in this for a people who reflect. (Qur'an, 45.13)".

I truly appreciate the efforts made by my supervisor, Professor Andris Kreicbergs to teach me science; his enthusiasm was beyond expectations

I cherish the company at work and leisure, and for the help in my project given by my colleagues in our lab., Dr. Tony Jian Li, Dr. Paul Ackermann and Dr. Daniel Bring

I am grateful to Dr. Mahmood Ahmed and Dr. Mariana Spetea, who taught me many practical aspects of research

I thank my collaborators from Endocrinology, Dr. Anna Ugarph-Morawski, Dr. Maria Sääf, Prof. Claes-Göran Östenson and Prof. Kerstin Brismar, Dr. Moira S. Lewitt and, from Gothenburg, Prof. Claes Ohlsson and, from Physiology, Dr. Indre-Bileviciute Ljungar for their essential contributions to my project

I appreciate the assistance and guidance from our laboratory staff, Ann-Britt Wikström, Liss Garberg, Barbro Granberg, Anja Finn, Ingrid Vedin and, from Gothenburg, Annette Hansevi for her expertise

I relish the company, encouragement and non-academic discussions and activities with my other colleagues in our research center, Ahmed Abdelaziz Ahmed, Dr. Monsur Kazi, Dr. Joy Roy, Dr. Hussam El-din El-nour, Dr. Yuji Yamamoto, Dr. Piotr Religa and Dr. Ozbek Emin

I appreciate the people at M3 Research Lab, K3 Surgical Sciences Administration and the animal lab. for the nice working atmosphere and professionalism

I am deeply grateful to Prof. Muhammad Umar, Prof. Mirza Rehman Beg, Prof. Mushtaq Ahmed, Prof. Roger Sutton from the Aga Khan University, Karachi, for their support of my doctoral studies, and for the other colleagues over there for their encouragement

I could not have completed my study without the support, understanding and prayers of my mother and brother, to whom I am deeply indebted

———————
———————
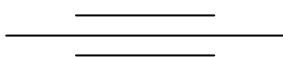
REFERENCES

1   Allgot B, Gan D, Alberti KGMM et al. *Diabetes Atlas.* 2000; Brussels: The International Diabetes Federation.

2   King H, Aubert RE & Herman WH Global burden of diabetes, 1995-2025: prevalence, numerical estimates, and projections. *Diabetes Care* 1998; **21**: 1414-31.

3   Green A, Christian Hirsch N & Krøger Pramming S The changing world demography of type 2 diabetes. *Diabetes/Metabolism Research and Reviews* 2003; **19**: 3-7.

4   The Cost of Diabetes. *Fact sheet No. 236.* Revised Sep. 2002; Brussels: World Health Organization.

5   Aubert RE, Ballard DJ, Bennett PH & Barrett-Connor E Diabetes in America:2nd Ed. 1995; Collindale, PA: DIANE Publishing Company

6   Vogt MT, Cauley JA, Tomaino MM, Stone K, Williams JR & Herndon JH Distal radius fractures in older women: a 10-year follow-up study of descriptive characteristics and risk factors. The study of osteoporotic fractures. *Journal of the American Geriatrics Society* 2002; **50**: 97-103.

7   Schwartz AV, Sellmeyer DE, Ensrud KE, Cauley JA, Tabor HK, Schreiner PJ, Jamal SA, Black DM & Cummings SR Older women with diabetes have an increased risk of fracture: a prospective study. *Journal of Clinical Endocrinology and Metabolism* 2001; **86**: 32-8.

8   Loder RT The influence of diabetes mellitus on the healing of closed fractures. *Clinical Orthopaedics and Related Research* 1988; **232**: 210-6.

9   Macey LR, Kana SM, Jingushi S, Terek RM, Borretos J & Bolander ME Defects of early fracture-healing in experimental diabetes. *Journal of Bone and Joint Surgery American Volume* 1989; **71**: 722-33.

10   Jeffcoate W, Lima J & Nobrega L The Charcot foot. *Diabetic Medicine* 2000; **17**: 253-8.

11   Alrefai H, Allababidi H, Levy S & Levy J The endocrine system in diabetes mellitus. *Endocrine* 2002; **18**: 105-19.

12   Krakauer JC, McKenna MJ, Buderer NF, Rao DS, Whitehouse FW & Parfitt AM Bone loss and bone turnover in diabetes. *Diabetes* 1995; **44**: 775-82.

13   Verhaeghe J, Visser WJ, Einhorn TA & Bouillon R Osteoporosis and diabetes: lessons from the diabetic BB rat. *Hormone Research* 1990; **34**: 245-8.

14   Rico H, Hernandez ER, Cabranes JA & Gomez-Castresana F Suggestion of a deficient osteoblastic function in diabetes mellitus: the possible cause of osteopenia in diabetics. *Calcified Tissue International* 1989; **45**: 71-3.

15   Hough FS Alterations of bone and mineral metabolism in diabetes mellitus. Part I. An overview. *South African Medical Journal* 1987; **72**: 116-9.

16   Ishida H, Seino Y, Taminato T, Usami M, Takeshita N, Seino Y, Tsutsumi C, Moriuchi S, Akiyama Y & Hara K Circulating levels and bone contents of bone gamma-carboxyglutamic acid-containing protein are decreased in streptozocin-induced diabetes. Possible marker for diabetic osteopenia. *Diabetes* 1988; **37**: 702-6.

17   Inaba M, Terada M, Koyama H, Yoshida O, Ishimura E, Kawagishi T, Okuno Y, Nishizawa Y, Otani S & Morii H Influence of high glucose on 1,25-dihydroxyvitamin D3-induced effect on human osteoblast-like MG-63 cells. *Journal of Bone and Mineral Research* 1995; **10**: 1050-6.

18   Blake GM & Fogelman I Dual energy x-ray absorptiometry and its clinical applications. *Seminars in Musculoskeletal Radiology* 2002; **6**: 207-18.

19   Tuominen JT, Impivaara O, Puukka P & Ronnemaa T Bone mineral density in patients with type 1 and type 2 diabetes. *Diabetes Care* 1999; **22**: 1196-200.

20   Bouillon R Diabetic bone disease. *Calcified Tissue International* 1991; **49**: 155-60.

21   Buysschaert M, Cauwe F, Jamart J, Brichant C, De Coster P, Magnan A & Donckier J Proximal femur density in type 1 and 2 diabetic patients. *Diabete and Metabolisme* 1992; **18**: 32-7.

22   Weiss RE & Reddi AH Influence of experimental diabetes and insulin on matrix-induced cartilage and bone differentiation. *American Journal of Physiology* 1980; **238**: E200-7.

23   Levin ME, Boisseau VC & Avioli LV Effects of diabetes mellitus on bone mass in juvenile and adult-onset diabetes. *New England Journal of Medicine* 1976; **294**: 241-5.

24   Seeman E Growth in bone mass and size--are racial and gender differences in bone mineral density more apparent than real? *Journal of Clinical Endocrinology and Metabolism* 1998; **83**: 1414-9.

25   Lu PW, Cowell CT, LLoyd-Jones SA, Briody JN & Howman-Giles R Volumetric bone mineral density in normal subjects, aged 5-27 years. *Journal of Clinical Endocrinology and Metabolism* 1996; **81**: 1586-90.

26   Seeman E Clinical review 137: Sexual dimorphism in skeletal size, density, and strength. *Journal of Clinical Endocrinology and Metabolism* 2001; **86**: 4576-84.

27   Lettgen B, Hauffa B, Möhlmann C, Jeken C & Reiners C Bone mineral density in children and adolescents with juvenile diabetes: selective measurement of bone mineral density of trabecular and cortical bone using peripheral quantitative computed tomography. *Hormone Research* 1995; **43**: 173-5.

28   Barrett-Connor E & Kritz-Silverstein D Does hyperinsulinemia preserve bone? *Diabetes Care* 1996; **19**: 1388-92.

29   Cornish J, Callon KE & Reid IR Insulin increases histomorphometric indices of bone formation In vivo. *Calcified Tissue International* 1996; **59**: 492-5.

30   Inaba M, Nishizawa Y, Shioi A & Morii H Importance of sustained high glucose condition in the development of diabetic osteopenia: possible involvement of the polyol pathway. *Osteoporosis International* 1997; **7 Suppl 3**: S209-12.

31   Terada M, Inaba M, Yano Y, Hasuma T, Nishizawa Y, Morii H & Otani S Growth-inhibitory effect of a high glucose concentration on osteoblast-like cells. *Bone* 1998; **22**: 17-23.

32   Yoshida O, Inaba M, Terada M, Shioi A, Nishizawa Y, Otani S & Morii H Impaired response of human osteosarcoma (MG-63) cells to human parathyroid hormone induced by sustained exposure to high glucose. *Mineral and Electrolyte Metabolism* 1995; **21**: 201-4.

33   Canalis E Effect of insulinlike growth factor I on DNA and protein synthesis in cultured rat calvaria. *Journal of Clinical Investigation* 1980; **66**: 709-19.

34   Hock JM, Centrella M & Canalis E Insulin-like growth factor I has independent effects on bone matrix formation and cell replication. *Endocrinology* 1988; **122**: 254-60.

35   McCarthy TL, Centrella M & Canalis E Regulatory effects of insulin-like growth factors I and II on bone collagen synthesis in rat calvarial cultures. *Endocrinology* 1989; **124**: 301-9.

REFERENCES

36   Mohan S & Baylink DJ Bone growth factors. *Clinical Orthopaedics and Related Research* 1991; **263**: 30-48.

37   Conover CA In vitro studies of insulin-like growth factor I and bone. *Growth Hormone and IGF Research* 2000; **10 Suppl B**: S107-10.

38   Daughaday WH & Rotwein P Insulin-like growth factors I and II. Peptide, messenger ribonucleic acid and gene structures, serum, and tissue concentrations. *Endocrine Reviews* 1989; **10**: 68-91.

39   Vignery A & McCarthy TL The neuropeptide calcitonin gene-related peptide stimulates insulin-like growth factor I production by primary fetal rat osteoblasts. *Bone* 1996; **18**: 331-5.

40   Woods KA, Camacho-Hubner C, Barter D, Clark AJ & Savage MO Insulin-like growth factor I gene deletion causing intrauterine growth retardation and severe short stature. *Acta Paediatrica Supplement* 1997; **423**: 39-45.

41   Zhang M, Xuan S, Bouxsein ML, von Stechow D, Akeno N, Faugere MC, Malluche H, Zhao G, Rosen CJ, Efstratiadis A et al. Osteoblast-specific knockout of the insulin-like growth factor (IGF) receptor gene reveals an essential role of IGF signaling in bone matrix mineralization. *Journal of Biological Chemistry* 2002; **277**: 44005-12.

42   Clemmons DR Role of insulin-like growth factor binding proteins in controlling IGF actions. *Molecular and Cellular Endocrinology* 1998; **140**: 19-24.

43   Mohan S, Nakao Y, Honda Y, Landale E, Leser U, Dony C, Lang K & Baylink DJ Studies on the mechanisms by which insulin-like growth factor (IGF) binding protein-4 (IGFBP-4) and IGFBP-5 modulate IGF actions in bone cells. *Journal of Biological Chemistry* 1995; **270**: 20424-31.

44   Miyakoshi N, Richman C, Kasukawa Y, Linkhart TA, Baylink DJ & Mohan S Evidence that IGF-binding protein-5 functions as a growth factor. *Journal of Clinical Investigation* 2001; **107**: 73-81.

45   Kanatani M, Sugimoto T, Nishiyama K & Chihara K Stimulatory effect of insulin-like growth factor binding protein-5 on mouse osteoclast formation and osteoclastic bone-resorbing activity. *Journal of Bone and Mineral Research* 2000; **15**: 902-10.

46   Bach LA & Rechler MM Insulin-like growth factors and diabetes. *Diabetes/metabolism Reviews* 1992; **8**: 229-57.

47   Hall K, Johansson BL, Póvoa G & Thalme B Serum levels of insulin-like growth factor (IGF) I, II and IGF binding protein in diabetic adolescents treated with continuous subcutaneous insulin infusion. *Journal of Internal Medicine* 1989; **225**: 273-8.

48   Edmonds ME, Roberts VC & Watkins PJ Blood flow in the diabetic neuropathic foot. *Diabetologia* 1982; **22**: 9-15.

49   Edmonds ME, Clarke MB, Newton S, Barrett J & Watkins PJ Increased uptake of bone radiopharmaceutical in diabetic neuropathy. *Quarterly Journal of Medicine* 1985; **57**: 843-55.

50   Gross TS, Damji AA, Judex S, Bray RC & Zernicke RF Bone hyperemia precedes disuse-induced intracortical bone resorption. *Journal of Applied Physiology* 1999; **86**: 230-5.

51   Laroche M Intraosseous circulation from physiology to disease. *Joint, Bone, Spine : Revue du Rhumatisme* 2002; **69**: 262-9.

52   Rajbhandari SM, Jenkins RC, Davies C & Tesfaye S Charcot neuroarthropathy in diabetes mellitus. *Diabetologia* 2002; **45**: 1085-96.

53 Wittenberg RH, Peschke U & Bötel U Heterotopic ossification after spinal cord injury. Epidemiology and risk factors. *Journal of Bone and Joint Surgery British Volume* 1992; **74**: 215-8.

54 Garland DE Clinical observations on fractures and heterotopic ossification in the spinal cord and traumatic brain injured populations. *Clinical Orthopaedics and Related Research* 1988; **233**: 86-101.

55 Mendelson L, Grosswasser Z, Najenson T, Sandbank U & Solzi P Periarticular new bone formation in patients suffering from severe head injuries. *Scandinavian Journal of Rehabilitation Medicine* 1975; **7**: 141-5.

56 Cundy TF, Edmonds ME & Watkins PJ Osteopenia and metatarsal fractures in diabetic neuropathy. *Diabetic Medicine* 1985; **2**: 461-4.

57 Carpintero P, Logroño C, Carreto A, Carrascal A & Lluch C Progression of bone lesions in cured leprosy patients. *Acta Leprologica* 1998; **11**: 21-4.

58 Bjurholm A, Kreicbergs A, Brodin E & Schultzberg M Substance P- and CGRP-immunoreactive nerves in bone. *Peptides* 1988; **9**: 165-71.

59 Bjurholm A, Kreicbergs A, Terenius L, Goldstein M & Schultzberg M Neuropeptide Y-, tyrosine hydroxylase- and vasoactive intestinal polypeptide-immunoreactive nerves in bone and surrounding tissue. *Journal of the Autonomic Nervous System* 1988; **25**: 119-25.

60 Bjurholm A Neuroendocrine peptides in bone. *International Orthopaedics* 1991; **15**: 325-9.

61 Kreicbergs A & Ahmed M Neuropeptides in bone. *Current Opinion in Orthopaedics* 1997; **8**: 71-9.

62 Mori T, Ogata T, Okumura H, Shibata T, Nakamura Y & Kataoka K Substance P regulates the function of rabbit cultured osteoclast; increase of intracellular free calcium concentration and enhancement of bone resorption. *Biochemical and Biophysical Research Communications* 1999; **262**: 418-22.

63 Sherman BE & Chole RA A mechanism for sympathectomy-induced bone resorption in the middle ear. *Otolaryngology - Head and Neck Surgery* 1995; **113**: 569-81.

64 Zaidi M, Alam AS, Bax BE, Shankar VS, Bax CM, Gill JS, Pazianas M, Huang CL, Sahinoglu T & Moonga BS Role of the endothelial cell in osteoclast control: new perspectives. *Bone* 1993; **14**: 97-102.

65 Cornish J, Callon KE, Bava U, Kamona SA, Cooper GJ & Reid IR Effects of calcitonin, amylin, and calcitonin gene-related peptide on osteoclast development. *Bone* 2001; **29**: 162-8.

66 Cornish J, Callon KE, Lin CQ, Xiao CL, Gamble GD, Cooper GJ & Reid IR Comparison of the effects of calcitonin gene-related peptide and amylin on osteoblasts. *Journal of Bone and Mineral Research* 1999; **14**: 1302-9.

67 Goto T, Yamaza T, Kido MA & Tanaka T Light- and electron-microscopic study of the distribution of axons containing substance P and the localization of neurokinin-1 receptor in bone. *Cell and Tissue Research* 1998; **293**: 87-93.

68 Bjurholm A, Kreicbergs A, Schultzberg M & Lerner UH Neuroendocrine regulation of cyclic AMP formation in osteoblastic cell lines (UMR-106-01, ROS 17/2.8, MC3T3-E1, and Saos-2) and primary bone cells. *Journal of Bone and Mineral Research* 1992; **7**: 1011-9.

69 Bjurholm A, Kreicbergs A, Schultzberg M & Lerner UH Parathyroid hormone and noradrenaline-induced enhancement of cyclic AMP in a cloned osteogenic sarcoma

cell line (UMR 106) is inhibited by neuropeptide Y. *Acta Physiologica Scandinavica* 1988; **134**: 451-2.

70   Hohmann EL, Levine L & Tashjian Jr AH Vasoactive intestinal peptide stimulates bone resorption via a cyclic adenosine 3',5'-monophosphate-dependent mechanism. *Endocrinology* 1983; **112**: 1233-9.

71   Lerner UH Neuropeptidergic regulation of bone resorption and bone formation. *Journal of Musculoskeletal and Neuronal Interactions* 2002; **2**: 440-7.

72   Baldock PA, Sainsbury A, Couzens M, Enriquez RF, Thomas GP, Gardiner EM & Herzog H Hypothalamic Y2 receptors regulate bone formation. *Journal of Clinical Investigation* 2002; **109**: 915-21.

73   Sherman BE & Chole RA In vivo effects of surgical sympathectomy on intramembranous bone resorption. *American Journal of Otology* 1996; **17**: 343-6.

74   Hill EL, Turner R & Elde R Effects of neonatal sympathectomy and capsaicin treatment on bone remodeling in rats. *Neuroscience* 1991; **44**: 747-55.

75   Downing JE & Miyan JA Neural immunoregulation: emerging roles for nerves in immune homeostasis and disease. *Immunology Today* 2000; **21**: 281-9.

76   Johnson RW, Arkins S, Dantzer R & Kelley KW Hormones, lymphohemopoietic cytokines and the neuroimmune axis. *Comparative Biochemistry and Physiology Part A, Physiology* 1997; **116**: 183-201.

77   Boulton AJ & Malik RA Diabetic neuropathy. *Medical Clinics of North America* 1998; **82**: 909-29.

78   Vinik AI, Park TS, Stansberry KB & Pittenger GL Diabetic neuropathies. *Diabetologia* 2000; **43**: 957-73.

79   Sima AA Pathological definition and evaluation of diabetic neuropathy and clinical correlations. *Canadian Journal of Neurological Sciences* 1994; **21**: S13-7.

80   Fernyhough P, Diemel LT, Brewster WJ & Tomlinson DR Deficits in sciatic nerve neuropeptide content coincide with a reduction in target tissue nerve growth factor messenger RNA in streptozotocin-diabetic rats: effects of insulin treatment. *Neuroscience* 1994; **62**: 337-44.

81   Robinson JP, Willars GB, Tomlinson DR & Keen P Axonal transport and tissue contents of substance P in rats with long-term streptozotocin-diabetes. Effects of the aldose reductase inhibitor 'statil'. *Brain Research* 1987; **426**: 339-48.

82   Levy DM, Karanth SS, Springall DR & Polak JM Depletion of cutaneous nerves and neuropeptides in diabetes mellitus: an immunocytochemical study. *Diabetologia* 1989; **32**: 427-33.

83   Ahlborg G & Lundberg JM Exercise-induced changes in neuropeptide Y, noradrenaline and endothelin-1 levels in young people with type I diabetes. *Clinical Physiology* 1996; **16**: 645-55.

84   Goto Y, Kakizaki M & Masaki N Production of spontaneous diabetic rats by repetition of selective breeding. *Tohoku Journal of Experimental Medicine* 1976; **119**: 85-90.

85   Ostenson CG The Goto-Kakizaki rat. In *Animal Models in Diabetes: A Primer (Frontiers in Animal Diabetes Research)*, pp197-211. Sima AAF & Shafrir E. 2001; Amsterdam: Harwood Academic Publishers.

86   Abdel-Halim SM, Guenifi A, Luthman H, Grill V, Efendic S & Ostenson CG Impact of diabetic inheritance on glucose tolerance and insulin secretion in spontaneously diabetic GK-Wistar rats. *Diabetes* 1994; **43**: 281-8.

87   Murakawa Y, Zhang W, Pierson CR, Brismar T, Ostenson CG, Efendic S & Sima AA Impaired glucose tolerance and insulinopenia in the GK-rat causes peripheral neuropathy. *Diabetes/Metabolism Research and Reviews* 2002; **18**: 473-83.

88   Peterson RG, Shaw WN, Neel M-A, Little LA & Eichberg J Zucker diabetic fatty rat as a model for non-insulin-dependent diabetes mellitus. *ILAR News (Inst Lab Animal Res)* 1990; **32**: 16-9.

89   Ostenson CG, Fière V, Ahmed M, Lindström P, Brismar K, Brismar T & Kreicbergs A Decreased cortical bone thickness in spontaneously non-insulin-dependent diabetic GK rats. *Journal of Diabetes and Its Complications* 1997; **11**: 319-22.

90   Centrala försöksdjursnämnden Euthanasia of experimental animals. EU-rapport om avlivning av försöksdjur. European Commission, DGXI. 1996; Stockholm: Regeringskansliets offsetcentral

91   Bertin E, Ruiz JC, Mourot J, Peiniau P & Portha B Evaluation of dual-energy X-Ray absorptiometry for body-composition assessment in rats. *Journal of Nutrition* 1998; **128**: 1550-4.

92   Mitlak BH, Schoenfeld D & Neer RM Accuracy, precision, and utility of spine and whole-skeleton mineral measurements by DXA in rats. *Journal of Bone and Mineral Research* 1994; **9**: 119-26.

93   Windahl SH, Vidal O, Andersson G, Gustafsson JA & Ohlsson C Increased cortical bone mineral content but unchanged trabecular bone mineral density in female ERbeta(-/-) mice. *Journal of Clinical Investigation* 1999; **104**: 895-901.

94   Vidal O, Lindberg MK, Hollberg K, Baylink DJ, Andersson G, Lubahn DB, Mohan S, Gustafsson JA & Ohlsson C Estrogen receptor specificity in the regulation of skeletal growth and maturation in male mice. *Proceedings of the National Academy of Sciences of the United States of America* 2000; **97**: 5474-9.

95   Tuukkanen J, Koivukangas A, Jämsä T, Sundquist K, Mackay CA & Marks SC Mineral density and bone strength are dissociated in long bones of rat osteopetrotic mutations. *Journal of Bone and Mineral Research* 2000; **15**: 1905-11.

96   McHugh NA, Vercesi HM, Egan RW & Hey JA In vivo rat assay: bone remodeling and steroid effects on juvenile bone by pQCT quantification in 7 days. *American Journal of Physiology Endocrinology and Metabolism* 2003; **284**: E70-5.

97   Louis O, Willnecker J, Soykens S, Van den Winkel P & Osteaux M Cortical thickness assessed by peripheral quantitative computed tomography: accuracy evaluated on radius specimens. *Osteoporosis International* 1995; **5**: 446-9.

98   Ferretti JL, Capozza RF & Zanchetta JR Mechanical validation of a tomographic (pQCT) index for noninvasive estimation of rat femur bending strength. *Bone* 1996; **18**: 97-102.

99   Sievanen H, Kannus P & Jarvinen M Precision of measurement by dual-energy X-ray absorptiometry of bone mineral density and content in rat hindlimb in vitro. *Journal of Bone and Mineral Research* 1994; **9**: 473-8.

100   Cummings SR, Bates D & Black DM Clinical use of bone densitometry: scientific review. *JAMA : the Journal of the American Medical Association* 2002; **288**: 1889-97.

101   Banse X, Devogelaer JP & Grynpas M Patient-specific microarchitecture of vertebral cancellous bone: a peripheral quantitative computed tomographic and histological study. *Bone* 2002; **30**: 829-35.

102   Banu MJ, Orhii PB, Mejia W, McCarter RJ, Mosekilde L, Thomsen JS & Kalu DN Analysis of the effects of growth hormone, voluntary exercise, and food restriction on diaphyseal bone in female F344 rats. *Bone* 1999; **25**: 469-80.

REFERENCES

103 Helterbrand JD, Higgs RE, Iversen PW, Tysarczyk-Niemeyer G & Sato M Application of automatic image segmentation to tibiae and vertebrae from ovariectomized rats. *Bone* 1997; **21**: 401-9.

104 Lu PW, Briody JN, Howman-Giles R, Trube A & Cowell CT DXA for bone density measurement in small rats weighing 150-250 grams. *Bone* 1994; **15**: 199-202.

105 Zamboni L & De Martino C Buffered picric acid-formaldehyde: A new, rapid fixative for electron microscopy. *Journal of Cell Biology* 1967; **35**: 148.

106 Bjurholm A, Kreicbergs A & Schultzberg M Fixation and demineralization of bone tissue for immunohistochemical staining of neuropeptides. *Calcified Tissue International* 1989; **45**: 227-31.

107 Ahmed M, Bjurholm A, Srinivasan GR, Theodorsson E, Kreicbergs A Extraction of neuropeptides from joint tissue for quantitation by radioimmunoassay. A study in the rat. *Peptides* 1994; **15**: 317-322.

108 Ahmed M, Srinivasan GR, Theodorsson E, Bjurholm A, Kreicbergs A Extraction and quantitation of neuropeptides in bone by radioimmunoassay. *Regul Pept* 1994; **51**: 179-188.

109 Brodin E, Nilsson G & Folkers K Characterization of two substance P antisera. *Acta Physiologica Scandinavica* 1982; **114**: 53-7.

110 Bang P, Eriksson U, Sara V, Wivall IL & Hall K Comparison of acid ethanol extraction and acid gel filtration prior to IGF-I and IGF-II radioimmunoassays: improvement of determinations in acid ethanol extracts by the use of truncated IGF-I as radioligand. *Acta Endocrinologica* 1991; **124**: 620-9.

111 Lewitt MS Stimulation of IGF-binding protein-1 secretion by AMP-activated protein kinase. *Biochemical and Biophysical Research Communications* 2001; **282**: 1126-31.

112 Chelius D & Spencer EM A new radioimmunoassay to measure rat insulin-like growth factor binding protein-4 (IGFBP-4) in serum, wound fluid and conditioned media. *Growth Hormone and IGF Research* 2001; **11**: 49-57.

113 Roach HI, Mehta G, Oreffo RO, Clarke NM & Cooper C Temporal analysis of rat growth plates: cessation of growth with age despite presence of a physis. *Journal of Histochemistry and Cytochemistry* 2003; **51**: 373-83.

114 Kilborn SH, Trudel G & Uhthoff H Review of growth plate closure compared with age at sexual maturity and lifespan in laboratory animals. *Contemporary Topics in Laboratory Animal Science* 2002; **41**: 21-6.

115 Walker KV & Kember NF Cell kinetics of growth cartilage in the rat tibia. II. Measurements during ageing. *Cell and Tissue Kinetics* 1972; **5**: 409-19.

116 Martin EA, Ritman EL & Turner RT Time course of epiphyseal growth plate fusion in rat tibiae. *Bone* 2003; **32**: 261-7.

117 Turner CH & Burr DB Basic biomechanical measurements of bone: a tutorial. *Bone* 1993; **14**: 595-608.

118 Seeman E From density to structure: growing up and growing old on the surfaces of bone. *Journal of Bone and Mineral Research* 1997; **12**: 509-21.

119 Ivers RQ, Cumming RG, Mitchell P & Peduto AJ Diabetes and risk of fracture: The Blue Mountains Eye Study. *Diabetes Care* 2001; **24**: 1198-203.

120 Hirano T, Burr DB, Turner CH, Sato M, Cain RL & Hock JM Anabolic effects of human biosynthetic parathyroid hormone fragment (1-34), LY333334, on remodeling and mechanical properties of cortical bone in rabbits. *Journal of Bone and Mineral Research* 1999; **14**: 536-45.

50

121   Young MJ, Marshall A, Adams JE, Selby PL & Boulton AJ Osteopenia, neurological dysfunction, and the development of Charcot neuroarthropathy. *Diabetes Care* 1995; **18**: 34-8.

122   Gough A, Abraha H, Li F, Purewal TS, Foster AV, Watkins PJ, Moniz C & Edmonds ME Measurement of markers of osteoclast and osteoblast activity in patients with acute and chronic diabetic Charcot neuroarthropathy. *Diabetic Medicine* 1997; **14**: 527-31.

123   Nelson DA & Jacober SJ Why do older women with diabetes have an increased fracture risk? *Journal of Clinical Endocrinology and Metabolism* 2001; **86**: 29-31.

124   Tobias JH, Flanagan AM & Scutt AM Novel therapeutic targets in osteoporosis. *Expert Opinions in Therapeutic Targets* 2002; **6**: 41-56.

125   Miyakoshi N, Qin X, Kasukawa Y, Richman C, Srivastava AK, Baylink DJ & Mohan S Systemic administration of insulin-like growth factor (IGF)-binding protein-4 (IGFBP-4) increases bone formation parameters in mice by increasing IGF bioavailability via an IGFBP-4 protease-dependent mechanism. *Endocrinology* 2001; **142**: 2641-8.

126   Zhang M, Faugere MC, Malluche H, Rosen CJ, Chernausek SD & Clemens TL Paracrine overexpression of IGFBP-4 in osteoblasts of transgenic mice decreases bone turnover and causes global growth retardation. *Journal of Bone and Mineral Research* 2003; **18**: 836-43.

127   Ishii DN Implication of insulin-like growth factors in the pathogenesis of diabetic neuropathy. *Brain Research Brain Research Reviews* 1995; **20**: 47-67.

128   Cacciatori V, Dellera A, Bellavere F, Bongiovanni LG, Teatini F, Gemma ML & Muggeo M Comparative assessment of peripheral sympathetic function by postural vasoconstriction arteriolar reflex and sympathetic skin response in NIDDM patients. *American Journal of Medicine* 1997; **102**: 365-70.

129   Meyer MF, Rose CJ, Hülsmann JO, Schatz H & Pfohl M Impaired 0.1-Hz vasomotion assessed by laser Doppler anemometry as an early index of peripheral sympathetic neuropathy in diabetes. *Microvascular Research* 2003; **65**: 88-95.

130   Wallengren J, Badendick K, Sundler F, Håkanson R & Zander E Innervation of the skin of the forearm in diabetic patients: relation to nerve function. *Acta Dermato-Venereologica* 1995; **75**: 37-42.

131   Lindblad BE, Nielsen LB, Jespersen SM, Bjurholm A, Bunger C & Hansen ES Vasoconstrictive action of neuropeptide Y in bone. The porcine tibia perfused in vivo. *Acta Orthopaedica Scandinavica* 1994; **65**: 629-34.

132   Lundberg P, Lie A, Bjurholm A, Lehenkari PP, Horton MA, Lerner UH & Ransjö M Vasoactive intestinal peptide regulates osteoclast activity via specific binding sites on both osteoclasts and osteoblasts. *Bone* 2000; **27**: 803-10.

133   Takeda S, Elefteriou F, Levasseur R, Liu X, Zhao L, Parker KL, Armstrong D, Ducy P & Karsenty G Leptin regulates bone formation via the sympathetic nervous system. *Cell* 2002; **111**: 305-17.

134   Cherruau M, Facchinetti P, Baroukh B & Saffar JL Chemical sympathectomy impairs bone resorption in rats: a role for the sympathetic system on bone metabolism. *Bone* 1999; **25**: 545-51.

APPENDIX A – TABULATED RESULTS

GLUCOSE TOLERANCE TEST

Table 5. Glucose tolerance test. Blood glucose level expressed as mean (mmol/L) ± SD at denoted time after glucose injection

	Control	**Diabetes**	**Difference (p-value)**
12 month	(n = 26)	(n = 23)	
Fasting	5.2 ± 0.9	9.1 ± 1.8	75% (*0.020*)
30 min	15.7 ± 2.8	24.7 ± 5.2	57% (*0.020*)
2 hour	5.7 ± 1.0	15.3 ± 3.8	169% (*<0.001*)
20 month	(n = 10)	(n = 10)	
Fasting	3.2 ± 0.3	4.4 ± 1.3	37% (*0.020*)
30 min	13.6 ± 6.9	21.7 ± 5.5	60% (*0.014*)
2 hour	8.5 ± 3.7	23.7 ± 6.3	178% (*<0.001*)

RADIOGRAPHY

Table 6. Diaphyseal characteristics of humerus and tibia from 12-month-old rats according to X-ray (mean ± SD)

	Control n=21	**Diabetes n=18**	**Difference (p-value)**
Humerus			
Periosteal diameter (mm)	2.3 ± 0.2	2.6 ± 0.2	10.3% (*<0.001*)
Endosteal diameter (mm)	0.9 ± 0.1	1.1 ± 0.1	23.2% (*<0.001*)
Cortical thickness (mm)	1.5 ± 0.1	1.5 ± 0.1	2.6% (0.447)
Cortical thickness index (periosteal/endosteal dia.)	2.7 ± 0.3	2.4 ± 0.2	-11.0% (*0.003*)
Tibia			
Periosteal diameter (mm)	2.0 ± 0.2	2.2 ± 0.1	7.2% (*0.004*)
Endosteal diameter (mm)	0.8 ± 0.1	0.9 ± 0.1	17.8% (*<0.001*)
Cortical thickness (mm)	1.3 ± 0.1	1.3 ± 0.1	1.0% (0.747)
Cortical thickness index (periosteal/endosteal dia.)	2.7 ± 0.2	2.5 ± 0.3	-8.9% (*0.008*)

DEXA

Table 7. *In-vivo* DEXA results from 12-month-old rats (mean ± SEM)

	Control n=21	Diabetes n=18	Difference (p-value)	
Bone Area				
WHOLE BODY (cm^2)	54.1 ± 0.9	50.7 ± 0.7	-6.3%	*(0.006)*
HUMERUS (mm^2)				
Prox. Metaphysis	29.9 ± 0.8	30.0 ± 0.9	0.1%	(0.973)
Diaphysis	11.0 ± 0.3	12.0 ± 0.2	8.9%	*(0.005)*
Dist. Metaphysis	24.1 ± 0.8	26.3 ± 1.0	9.3%	(0.080)
TIBIA (mm^2)				
Prox. Metaphysis	25.2 ± 0.7	25.6 ± 0.6	1.9%	(0.597)
Diaphysis	13.7 ± 0.3	14.3 ± 0.2	4.1%	(0.163)
Dist. Metaphysis	19.2 ± 2.6	18.6 ± 0.5	-3.2%	(0.821)
VERTEBRAE (mm^2)	89.5 ± 3	80.3 ± 2.1	-10.3%	*(0.015)*
Bone Mineral Content				
WHOLE BODY (g)	10.7 ± 0.3	9.8 ± 0.1	-8.3%	*(0.004)*
HUMERUS (mg)				
Prox. Metaphysis	91.9 ± 3.6	78.2 ± 3.0	-14.9%	*(0.006)*
Diaphysis	34.0 ± 1.1	34.3 ± 1.0	1%	(0.818)
Dist. Metaphysis	79.1 ± 3.3	74.8 ± 3.0	-5.5%	(0.333)
TIBIA (mg)				
Prox. Metaphysis	70.4 ± 2.3	64.9 ± 1.2	-7.7%	*(0.032)*
Diaphysis	43.4 ± 1.2	49 ± 1.1	12.9%	*(0.001)*
Dist. Metaphysis	64.7 ± 8.4	60.5 ± 2.5	-6.4%	(0.637)
VERTEBRAE (mg)	230.6 ± 13.1	157.3 ± 7.0	-31.8%	*(<0.001)*
Bone Mineral Density				
WHOLE BODY (mg/cm^2)	198 ± 3	194 ± 4	-1.8%	(0.472)
HUMERUS (mg/cm^2)				
Prox. Metaphysis	306 ± 7	261 ± 4	-14.9%	*(<0.001)*
Diaphysis	309 ± 6	286 ± 6	-7.4%	*(0.009)*
Dist. Metaphysis	328 ± 6	286 ± 8	-12.9%	*(<0.001)*
TIBIA (mg/cm^2)				
Prox. Metaphysis	285 ± 5	254 ± 5	-11%	*(<0.001)*
Diaphysis	316 ± 5	343 ± 6	8.6%	*(0.002)*
Dist. Metaphysis	337 ± 5	324 ± 11	-4%	(0.271)
VERTEBRAE (mg/cm^2)	255 ± 8	196 ± 6	-23.3%	*(<0.001)*

Table 8. *Ex-vivo* DEXA results from 12-month-old rats (mean ± SD)

		Control n=5	Diabetes n=5	Difference (p-value)	
BONE AREA (cm²)					
Whole body		59.6 ± 4.68	55.8 ± 4.57	-6.5%	(0.2232)
	Whole	1.12 ± 0.09	0.88 ± 0.06	-21.1%	*(0.0011)*
Humerus	Metaphysis	0.50 ± 0.04	0.39 ± 0.03	-22.9%	*(0.0009)*
	Diaphysis	0.21 ± 0.02	0.18 ± 0.01	-17.1%	*(0.0135)*
	Whole	1.42 ± 0.06	1.32 ± 0.06	-7.2%	*(0.0279)*
Tibia	Metaphysis	0.70 ± 0.03	0.59 ± 0.04	-15.8%	*(0.0005)*
	Diaphysis	0.17 ± 0.01	0.18 ± 0.01	8.1%	*(0.0019)*
	Whole	0.31 ± 0.02	0.34 ± 0.04	7.9%	(0.2208)
Metatarsal	Metaphysis	0.10 ± 0.01	0.11 ± 0.01	16.1%	*(0.0491)*
	Diaphysis	0.11 ± 0.01	0.11 ± 0.02	3.4%	(0.6635)
Vertebrae		1.09 ± 0.08	0.82 ± 0.08	-24.5%	*(0.0008)*
BMC (mg)					
Whole body		11.4 ± 1.0	10.1 ± 0.8	-12.0%	*(0.0373)*
	Whole	211.9 ± 35.8	153.3 ± 15.1	-23.7%	*(0.0011)*
Humerus	Metaphysis	91.2 ± 6.0	63.2 ± 7.5	-30.7%	*(0.0002)*
	Diaphysis	35.8 ± 3.9	30.1 ± 2.1	-16.0%	*(0.0203)*
	Whole	300.7 ± 26.1	245.6 ± 22.3	-18.3%	*(0.0071)*
Tibia	Metaphysis	161.7 ± 16.5	108.8 ± 9.9	-32.7%	*(0.0003)*
	Diaphysis	31.8 ± 1.9	36.1 ± 3.2	13.8%	*(0.0309)*
	Whole	25.0 ± 1.9	27.4 ± 3.2	9.4%	(0.1994)
Metatarsal	Metaphysis	8.5 ± 0.8	8.6 ± 1.5	0.5%	(0.9573)
	Diaphysis	7.4 ± 0.6	9.0 ± 1.2	20.6%	*(0.0290)*
Vertebrae		276.1 ± 37.2	169.2 ± 19.4	-38.7%	*(0.0005)*
BMD (mg/cm²)					
Whole body		192.0 ± 14.82	180.4 ± 4.96	-6.0%	(0.1369)
	Whole	180.4 ± 11.4	173.9 ± 6.8	-3.6%	(0.3028)
Humerus	Metaphysis	179.6 ± 11.8	162.3 ± 8.3	-9.6%	*(0.0281)*
	Diaphysis	170.7 ± 12.9	172.4 ± 4.1	1.0%	(0.7777)
	Whole	211.7 ± 10.0	186.3 ± 8.7	-12.0%	*(0.0027)*
Tibia	Metaphysis	229.6 ± 14.9	183.6 ± 6.5	-20.0%	*(0.0002)*
	Diaphysis	186.1 ± 5.8	195.9 ± 14.8	5.2%	(0.2055)
	Whole	80.5 ± 3.1	81.6 ± 1.6	1.4%	(0.4944)
Metatarsal	Metaphysis	78.4 ± 2.3	75.9 ± 3.9	-3.2%	(0.2532)
	Diaphysis	79.2 ± 5.5	81.6 ± 1.8	3.1%	(0.3726)
Vertebrae		252.5 ± 21.4	205.5 ± 8.9	-18.6%	*(0.0019)*

Table 9. *Ex-vivo* **DEXA results from 20-month-old rats (mean ± SD)**

	Control n=10	Diabetes n=10	Difference (p-value)
Length (mm)			
TIBIA	47.1 ± 2.1	46.3 ± 0.8	-1.8% (0.256)
METATARSAL	16.3 ± 0.4	16.2 ± 0.4	~0% (0.673)
Bone Area (cm^2)			
TIBIA			
Whole bone	2.783 ± 0.227	2.772 ± 0.060	-0.4% (0.878)
Metaphysis	0.837 ± 0.054	0.757 ± 0.014	-9.6% (*<.001*)
Diaphysis	0.339 ± 0.016	0.368 ± 0.010	8.5% (*<.001*)
METATARSAL			
Whole bone	0.332 ± 0.021	0.340 ± 0.022	2.4% (0.420)
Metaphysis	0.116 ± 0.009	0.113 ± 0.014	-2.6% (0.577)
Diaphysis	0.108 ± 0.007	0.117 ± 0.006	9.0% (*0.005*)
BMC (mg)			
TIBIA			
Whole bone	505.8 ± 69.1	437.3 ± 21.9	-13.6% (*0.008*)
Metaphysis	164.6 ± 26.1	112.3 ± 7.8	-31.8% (*<.001*)
Diaphysis	57.6 ± 7.2	61.7 ± 4.6	7.2% (0.141)
METATARSAL			
Whole bone	34.0 ± 2.9	33.5 ± 2.2	-1.3% (0.708)
Metaphysis	11.3 ± 1.1	10.1 ± 1.2	-11.2% (*0.024*)
Diaphysis	10.6 ± 1.0	11.5 ± 0.6	7.9% (*0.041*)
BMD (mg/cm^2)			
TIBIA			
Whole bone	181.2 ± 12.4	157.8 ± 6.2	-12.9% (*<.001*)
Metaphysis	195.7 ± 20.1	148.3 ± 9.0	-24.3% (*<.001*)
Diaphysis	169.2 ± 13.4	167.6 ± 8.9	-1.0% (0.751)
METATARSAL			
Whole bone	102.1 ± 3.4	98.5 ± 1.5	-3.5% (*0.007*)
Metaphysis	97.3 ± 4.8	88.8 ± 2.4	-8.8% (*<.001*)
Diaphysis	98.5 ± 4.2	97.8 ± 2.6	~0% (0.622)

ASH WEIGHT

Table 10. Ash weight results from 12-month-old rats (mean ± SD)

	Control n=5	Diabetes n=5	Difference (p-value)
Ash Weight (mg)			
TIBIA			
Whole bone	321.1 ± 23.91	262.1 ± 18.89	-18.4% *(0.0025)*
Prox. Metaphysis	166.2 ± 16.54	110.5 ± 7.71	-33.5% *(0.0001)*
Diaphysis	50.1 ± 5.14	52.5 ± 3.41	4.9% (0.4019)
Dist. Metaphysis	36.8 ± 4.63	35.1 ± 2.6	-4.7% (0.4891)
HUMERUS			
Whole bone	203.6 ± 14.45	161.0 ± 14.62	-20.9% *(0.0017)*
Prox. Metaphysis	101.6 ± 9.74	76.9 ± 8.45	-24.3% *(0.0027)*
Diaphysis	45.4 ± 4.48	38.5 ± 4.06	-15.2% *(0.0343)*
Dist. Metaphysis	56.6 ± 2.95	45.5 ± 3.77	-19.5% 0.0009)
METATARSAL	23.6 ± 1.02	24.4 ± 2.10	3.5% (0.4546)
VERTEBRAE	256.2 ± 40.19	173.9 ± 10.81	-32.1% *(0.0022)*
Percent Ash (Ash wt/ dry bone wt)			
TIBIA			
Whole bone	62.3 ± 0.83	61.8 ± 0.51	-0.5% (0.2872)
Prox. Metaphysis	60.1 ± 1.19	57.9 ± 0.85	-2.2% (0.0109)
Diaphysis	67.1 ± 0.49	66.3 ± 0.23	-0.7% (0.0151)
Dist. Metaphysis	58.8 ± 1.32	61.1 ± 0.84	2.3% (0.0116)
HUMERUS			
Whole bone	62.0 ± 1.14	61.8 ± 0.87	-0.1% (0.8214)
Prox. Metaphysis	59.8 ± 1.43	59.6 ± 0.9	-0.2% (0.8312)
Diaphysis	66.2 ± 1.99	65.6 ± 1.11	-0.6% (0.6020)
Dist. Metaphysis	62.9 ± 1.81	62.6 ± 1.88	-0.3% (0.7854)
METATARSAL	59.9 ± 0.82	62.9 ± 1.11	3.0% (0.0013)
VERTEBRAE	55.6 ± 2.08	56.8 ± 0.63	1.2% (0.2592)

Table 11. Ash weight results from 20-month-old rats (mean ± SD)

	Control n=10	Diabetes n=10	Difference (p-value)
Ash Weight (mg)			
TIBIA			
Whole bone	507.5 ± 68.3	438.7 ± 20.9	-13.6% (*0.007*)
Metaphysis	158.7 ± 20.0	97.5 ± 9.5	-38.6% (*<.001*)
Diaphysis	81.0 ± 12.4	81.5 ± 9.1	0.6% (0.926)
METATARSAL	34.1 ± 3.0	32.3 ± 1.4	-5.3% (0.107)
Percent Ash (Ashwt/ dry bone wt)			
TIBIA			
Whole bone	62.9 ± 1.3	61.2 ± 0.9	-2.7% (*0.002*)
Metaphysis	56.2 ± 2.3	51.5 ± 2.0	-8.3% (*<.001*)
Diaphysis	68.1 ± 1.1	67.1 ± 0.9	-1.4% (*0.040*)
METATARSAL	62.7 ± 1.2	60.2 ± 1.3	-3.9% (*<.001*)

Table 12. Correlation between ash weight and BMC for bones from 12-month-old rats expressed as Pearson's correlation coefficient r (p-value).

	Control n=5	Diabetes n=5
Tibia	0.974 (*0.005*)	0.984 (*0.002*)
Humerus	0.938 (*0.018*)	0.912 (*0.031*)
Metatarsal	0.623 (0.262)	0.933 (*0.021*)
Vertebrae	0.867 (0.057)	0.989 (*<.001*)

Table 13. Correlation between ash weight and BMC for bones from 20-month-old rats expressed as Pearson's correlation coefficient r (p-value).

	Control n=10	Diabetes n=10
Tibia	0.984 (*<.001*)	0.931 (*<.001*)
Metatarsal	0.966 (*<.001*)	0.900 (*<.001*)

PQCT

Table 14. Size and form of bones from 12-month-old rats (mean ± SD)

	Control n=5	Diabetes n=5	Difference (p-value)
Length (mm)			
Humerus	29.7 ± 0.76	27.4 ± 0.82	-7.7% *(0.0018)*
Tibia	40.6 ± 0.72	39.7 ± 0.95	-2.3% (0.1150)
Metatarsal	15.8 ± 0.17	16.2 ± 0.32	+2.9% *(0.0214)*
Vertebral body L4,L5	6.3 ± 0.28	5.8 ± 0.17	-7.9% *(0.0083)*
Cross-Sectional Area (mm^2)			
Humerus Metaphysis	8.66 ± 0.932	7.80 ± 0.348	-9.9% (0.0912)
Diaphysis	4.71 ± 0.273	5.31 ± 0.265	+12.7% *(0.0078)*
Tibia Metaphysis	17.91 ± 1.582	13.23 ± 0.270	-26.1% *(0.0002)*
Diaphysis	4.90 ± 0.172	5.61 ± 0.241	+14.4% *(0.0007)*
Metatarsal Diaphysis	1.45 ± 0.091	1.68 ± 0.017	+15.3% *(0.0007)*
Vertebral Endplate	6.93 ± 0.625	6.28 ± 0.360	-9.5% (0.0768)
Body Middle	6.16 ± 0.550	6.11 ± 0.210	-0.9% (0.8420)
Circumferences (mm) -diaphysis			
Humerus Periosteal	7.69 ± 0.224	8.16 ± 0.203	+6.2% *(0.0078)*
Endosteal	3.09 ± 0.167	3.55 ± 0.104	+14.7% *(0.0008)*
Tibia Periosteal	7.85 ± 0.138	8.39 ± 0.181	+6.9% *(0.0007)*
Endosteal	3.74 ± 0.224	3.85 ± 0.134	+3.0% (0.3714)
Metatarsal Periosteal	4.27 ± 0.132	4.59 ± 0.023	+7.4% *(0.0007)*
Endosteal	1.96 ± 0.134	2.29 ± 0.026	+16.9% *(0.0006)*
Cortical thickness (mm) -diaphysis			
Humerus	0.73 ± 0.026	0.73 ± 0.042	+0.4% (0.8889)
Tibia	0.66 ± 0.036	0.72 ± 0.027	+10.5% *(0.0092)*
Metatarsal	0.37 ± 0.004	0.37 ± 0.006	-0.6% (0.5163)

Table 15. Volumetric mineral density (mg/cm^3) of bones from 12-month-old rats according to pQCT (mean ± SD)

		Control n=5	Diabetes n=5	Difference (p-value)	
Total-metaphyseal					
	Humeral metaphysis	758.4 ± 77.26	655.8 ± 17.94	-13.5%	(0.0201)
	Tibial metaphysis	682.6 ± 65.83	613.5 ± 29.88	-10.1%	(0.0650)
Vertebral	End plate	747.1 ± 74.92	600.0 ± 47.50	-19.7%	(0.0060)
Body	Middle	666.2 ± 73.04	517.2 ± 26.43	-22.4%	(0.0027)
Trabecular-metaphyseal					
	Humeral metaphysis	339.2 ± 81.74	160.6 ± 33.36	-52.7%	(0.0019)
	Tibial metaphysis	431.9 ± 90.07	272.5 ± 32.23	-36.9%	(0.0058)
Vertebral	End plate	576.5 ± 79.01	383.2 ± 58.88	-33.5%	(0.0023)
Body	Middle	459.8 ± 75.10	269.1 ± 18.24	-41.5%	(0.0006)
Cortical-diaphyseal					
	Humerus	1437.3 ± 5.74	1399.1 ± 16.35	-2.7%	(0.0012)
	Tibia	1331.3 ± 9.36	1314.6 ± 22.04	-1.2%	(0.1593)
	Metatarsal	1277.9 ± 12.11	1281.8 ± 7.42	+0.3%	(0.5504)

Table 16. Estimated strength of diaphysis of long bones from 12-month-old rats (mean ± SD)

	Control n=5	Diabetes n=5	Difference (p-value)
Cross-sectional moment of inertia (mm^4)			
Humerus	3.96 ± 0.436	5.52 ± 0.672	+39.5% (0.0024)
Tibia	3.84 ± 0.297	5.56 ± 0.565	+44.9% (0.0003)
Metatarsal	0.29 ± 0.033	0.37 ± 0.011	+29.9% (0.0005)
Bone strength index (mm^4.g/cm^3)			
Humerus	5.68 ± 0.615	7.72 ± 0.989	+35.9% (0.0045)
Tibia	5.11 ± 0.402	7.31 ± 0.692	+43.0% (0.0003)
Metatarsal	0.37 ± 0.042	0.48 ± 0.016	+30.3% (0.0006)

Table 17. pQCT results from 20-month-old rats (mean ± SD)

	Control n=10	Diabetes n=10	Difference (p-value)	
Tibial Metaphysis				
Cross-sectional area (mm^2)	26.11 ± 2.95	20.81 ± 0.74	-20.3%	(*<.001*)
Total BMD (g/cm^3)	0.541 ± 0.050	0.408 ± 0.029	-24.6%	(*<.001*)
Trabecular BMD (g/cm^3)	0.284 ± 0.051	0.108 ± 0.038	-61.9%	(*<.001*)
Tibial Diaphysis				
Periosteal circumference (mm)	9.44 ± 0.46	10.22 ± 0.21	8.3%	(*<.001*)
Endosteal circumference (mm)	4.18 ± 0.26	4.93 ± 0.16	17.9%	(*<.001*)
Cross-sec. moment of inertia (mm^4)	8.41 ± 1.73	12.08 ± 1.07	43.6%	(*0.001*)
Cortical BMD (g/cm^3)	1.42 ± 0.01	1.42 ± 0.01	≈0	(0.763)
Cortical thickness (mm)	0.84 ± 0.06	0.84 ± 0.03	≈0	(0.859)
Metatarsal Diaphysis				
Periosteal circumference (mm)	4.88 ± 0.18	5.04 ± 0.07	3.4%	(*0.016*)
Endosteal circumference (mm)	2.15 ± 0.15	2.46 ± 0.09	14.3%	(*<.001*)
Cross-sec. moment of inertia (mm^4)	0.51 ± 0.08	0.58 ± 0.04	13.0%	(*0.029*)
Cortical BMD (g/cm^3)	1.38 ± 0.01	1.38 ± 0.02	≈0	(0.920)
Cortical thickness (mm)	0.43 ± 0.01	0.41 ± 0.01	-5.3%	(*<.001*)

IMMUNOASSAY

Table 18. Tissue IGF-I in 12-month-old rats according to RIA (mean ± SEM)

	Control n=15	Diabetes n=15	Difference (p-value)	
Tissue (µg/mg)				
Cortical bone	219 ± 55	135 ± 47	-38.3%	(*<0.001*)
Ankle	161 ± 42	165 ± 32	2.7%	(0.766)

APPENDIX B – PAPERS

PAPER I

Ahmad T, Ohlsson C, Ostenson CG, Kreicbergs A. Peripheral quantitative computed tomography for the detection of diabetic osteopathy. A study in the Goto-Kakizaki rat. Invest Radiol 2003; 38:171-176.

PAPER II

Ahmad T, Ohlsson C, Sääf M, Östenson C-G, Kreicbergs A. Skeletal changes in the type-2 diabetic Goto-Kakizaki rat. J Endocrinol 2003; 178:111-116

PAPER III

Ahmad T, Ugarph-Morawski A, Lewitt MS, Li J, Sääf M, Brismar K. Diabetic osteopathy and the IGF system in the Goto-Kakizaki rat. Submitted; Aug 2003

PAPER IV

Ahmad T, Ugarph-Morawski A, Li J, Indre-Bileviciute-Ljungar, Anja Finn, Östenson C-G, Kreicbergs A. Bone and joint neuropathy in rats with type-2 diabetes. Submitted; Aug 2003